OPEN

Role of ADAMTS-5 in Aortic Dilatation and Extracellular Matrix Remodeling

Marika Fava, Javier Barallobre-Barreiro, Ursula Mayr, Ruifang Lu, Athanasios Didangelos, Ferheen Baig, Marc Lynch, Norman Catibog, Abhishek Joshi, Temo Barwari, Xiaoke Yin, Marjan Jahangiri, Manuel Mayr

Objective—Thoracic aortic aneurysm (TAA), a degenerative disease of the aortic wall, is accompanied by changes in the structure and composition of the aortic ECM (extracellular matrix). The ADAMTS (a disintegrin and metalloproteinase with thrombospondin motifs) family of proteases has recently been implicated in TAA formation. This study aimed to investigate the contribution of ADAMTS-5 to TAA development.

Approach and Results—A model of aortic dilatation by AngII (angiotensin II) infusion was adopted in mice lacking the catalytic domain of ADAMTS-5 (Adamts5$^{\Delta cat}$). Adamts5$^{\Delta cat}$ mice showed an attenuated rise in blood pressure while displaying increased dilatation of the ascending aorta (AsAo). Interestingly, a proteomic comparison of the aortic ECM from AngII-treated wild-type and Adamts5$^{\Delta cat}$ mice revealed versican as the most upregulated ECM protein in Adamts5$^{\Delta cat}$ mice. This was accompanied by a marked reduction of ADAMTS-specific versican cleavage products (versikine) and a decrease of LRP1 (low-density lipoprotein-related protein 1). Silencing *LRP1* expression in human aortic smooth muscle cells reduced the expression of *ADAMTS5*, attenuated the generation of versikine, but increased soluble ADAMTS-1. A similar increase in ADAMTS-1 was observed in aortas of AngII-treated Adamts5$^{\Delta cat}$ mice but was not sufficient to maintain versican processing and prevent aortic dilatation.

Conclusions—Our results support the emerging role of ADAMTS proteases in TAA. ADAMTS-5 rather than ADAMTS-1 is the key protease for versican regulation in murine aortas. Further studies are needed to define the ECM substrates of the different ADAMTS proteases and their contribution to TAA formation.

Visual Overview—An online visual overview is available for this article. (*Arterioscler Thromb Vasc Biol*. 2018;38: 1537-1548. DOI: 10.1161/ATVBAHA.117.310562.)

Key Words: aneurysm ■ aorta ■ extracellular matrix ■ proteases ■ proteomics

ECM (extracellular matrix) degradation and remodeling is a hallmark of aortic aneurysm formation. The precise mechanisms behind the degradation of ECM components and subsequent dissection of the vessel wall are not completely elucidated. Histologically, diseased aortas present with variable degrees of ECM degeneration within the aortic medial layer, including cystic medial degeneration, elastic fiber fragmentation, and myxomatous degeneration. At the molecular level, aortic degeneration has been associated with vascular smooth muscle cell (SMC) apoptosis[1] and inflammation.[2] Factors that contribute to aortic wall degeneration both in humans and in animal models include AngII (angiotensin II),[3] TGF-β (transforming growth factor-β),[4] and MMPs (matrix metalloproteinases).[5] The role of MMPs in the alteration of aortic ECM architecture has been extensively studied in the context of aortic aneurysm development.[5,6] More recently, a family of metalloproteinases known as ADAMTSs

(a disintegrin and metalloproteinase with thrombospondin motifs) has been explored in vascular ECM turnover. In particular, ADAMTS-1, -4, and -5 activities have been implicated in thoracic aortic aneurysm (TAA) formation.[3,7,8]

See accompanying editorial on page 1425

ADAMTS-1, -4, and -5 are the main enzymes responsible for large aggregating proteoglycan cleavage.[9,10] We have previously demonstrated that ADAMTS-5 is reduced in aortas of apolipoprotein E–null mice and that ADAMTS-5 activity affects proteoglycan-mediated lipoprotein retention.[11] We have also shown that on stent-induced vascular injury, a reduction in ADAMTS-1 and ADAMTS-5 contributes to an accumulation of large aggregating proteoglycans, notably aggrecan and versican.[12] Similarly, the absence of ADAMTS-5 leads to developmental defects including myxomatous valve malformation. Mice lacking ADAMTS-5 activity cannot degrade

Nonstandard Abbreviations and Acronyms	
ADAMTS	a disintegrin and metalloproteinase with thrombospondin motifs
AngII	angiotensin II
AsAo	ascending aorta
CO6A6	collagen type VI α-6
COCA1	collagen type XII α-1
ECM	extracellular matrix
FINC	fibronectin
GuHCl	guanidine hydrochloride
LRP1	low-density lipoprotein-related protein 1
MFAP5	microfibrillar-associated protein 5
MMPs	matrix metalloproteinases
SDS	sodium dodecyl sulfate
SMCs	smooth muscle cells
TAA	thoracic aortic aneurysm
TGF-β	transforming growth factor-β

versican during the remodeling of the valve cushion resulting in enlarged pulmonary and aortic valve cusps.[13] LRP1 (low-density lipoprotein-related protein 1), a widely expressed receptor, is known to mediate ADAMTS-5 clearance by promoting its endocytosis. Interestingly, LRP1 has been implicated in aneurysm formation; LRP1 deletion in SMCs profoundly augmented aneurysm formation in the ascending aorta (AsAo) induced by AngII.[14]

In the present article, we aim to characterize regional differences in ADAMTS expression in murine aortas and to explore aortic ECM changes in mice with loss of ADAMTS-5 activity. Because the ECM is an intricate protein network and alterations in proteolytic activity will induce secondary remodeling processes, we used our established proteomics approach for studying the vascular ECM.[15]

Materials and Methods

An expanded Materials and Methods section is available in the online-only Data Supplement. The data that support the findings of this study are available from the corresponding author on reasonable request. The proteomics data, however, are deposited to the ProteomeXchange Consortium via the PRIDE partner repository with the dataset identifier PXD009410 and 10.6019/PXD009410.

Animal Experiments

All animal procedures were performed by authorized researchers in the Cardiovascular Division, King's College London. Housing and animal care was in accordance with the UK Animals (Scientific Procedures) Act 1986. Genotyping of Adamts5$^{\Delta cat}$ and control (Adamts5$^{+/+}$) mice was performed as previously published.[11] For AngII infusion, osmotic mini-pumps (Alzet, model 1004) containing AngII (1.44 mg g^{-1} d^{-1} dissolved in saline) were implanted in 10- to 12-week-old male Adamts5$^{\Delta cat}$ and Adamts5$^{+/+}$ mice derived from littermates of heterozygous breeders (JAX stock no. 005771, B6.129P2-*Adamts5*^{tm1Dgen}/J). Animals were euthanized after 4 weeks, and the entire aorta was excised and immediately washed in sterile phosphate-buffered saline. The entire aorta was snap-frozen at −80°C for subsequent proteomic analysis. For gene expression analysis, aortic tissue was divided into anatomically defined regions using a scalpel under a dissecting microscope, followed by immediate storage at −80°C. Aortic diameter was monitored using ultrasound at day 0 (baseline) and after 27 days of AngII treatment using Vevo software version 1.7.

Mouse Echocardiography

Animals were anesthetized using 5% isoflurane mixed with 1 L/min of 100% oxygen for 45 seconds to 1 minute. Mice were then placed in a supine position on a heating pad with embedded ECG registration. On adequate induction, 1% to 1.5% isoflurane mixed with 1 L/min 100% oxygen was used to maintain a steady state of sedation throughout the procedure. A rectal probe was inserted to continuously monitor the body temperature. Electrode gel was applied to the 4 paws, which were taped to the ECG electrodes. Two-dimensional echocardiographic images of cardiovascular anatomy were obtained by a single operator. Standard and modified parasternal long-axis, suprasternal, longitudinal abdominal, and transverse abdominal views were obtained using Visual Sonics Vevo 2100. Aortic root dimensions (aortic annulus, sinuses of Valsalva, and sinotubular junction) were measured in parasternal long-axis view. AsAo dimensions were measured during systole and diastole in suprasternal view where possible and modified parasternal long-axis view if suprasternal views were considered inadequate. Measurements were taken from leading edge-to-leading edge. Abdominal aorta measurements were made in the transverse abdominal view. All measurements were performed offline (Vevo software version 1.7) by 2 consensus interpreters.

Blood Pressure Monitoring

The blood pressure was directly measured via an implantable radio-telemetry device. An average of 200 values were acquired every 5 minutes for 18 to 20 hours. Blood pressure was monitored using telemetry probes 2 days before mini-pump implantation and at days 5 and 27 of AngII infusion.

ECM Protein Extraction From Murine Aortas

Aortic samples were partially thawed and diced into smaller pieces to aid the removal of plasma contaminants and for the effective extraction of ECM proteins.[16,17] ECM protein enrichment of aortic samples was performed using an adaptation of our previously published 3-step extraction method, involving sequential incubation with 0.5 mol/L NaCl for 2 hours, 0.08% sodium dodecyl sulfate (SDS) for 2 hours, and a final incubation with 4 mol/L guanidine hydrochloride (GuHCl) for 48 hours. After precipitation of GuHCl extracts, protein samples were enzymatically deglycosylated and subjected to in-solution trypsin digestion. Details are given in Online Methods in the online-only Data Supplement.

Proteomics Analysis of ECM Extracts

After deglycosylation (protocol details are provided in the Online Methods in the online-only Data Supplement), digested peptides were separated on a nanoflow liquid chromatography system, and GuHCl extracts were injected for liquid chromatography-tandem mass spectrometry analysis into a Q Exactive HF Hybrid Quadrupole-Orbitrap mass spectrometer (Thermo Fisher Scientific) for discovery proteomics. Acquisition was performed as previously described.[15] For targeted MS analysis, a precursor isolation list was created for proteotypic peptides of mouse versican and GuHCl extracts were analyzed via parallel reaction monitoring mode on a Q Exactive HF Hybrid Quadrupole-Orbitrap mass spectrometer. Details are given in Online Methods in the online-only Data Supplement.

Total Protein Extraction From Murine Aortas

Mouse aortic samples were homogenized in the presence of 300 μL of tissue lysis buffer (0.152 g of Tris, 0.33 g of NaCl, 0.038 g of EGTA, 0.073 g of EDTA, 500 μL of Triton X-100, and 250 μL of 20% SDS) at pH 7.4. Protein concentration was measured using the Pierce BCA Protein Assay Kit, and Western blots were performed following the protocol in the Online Methods in the online-only Data Supplement.

Cell Culture of Human Arterial SMCs

Samples of internal mammary artery were collected from patients undergoing bypass graft surgery at Leeds General Infirmary,

conforming with the principles outlined in the Declaration of Helsinki. Arterial SMCs were extracted and expanded using an explant technique.[18] SMCs were seeded into 6-well tissue culture plates. Twenty-four hours after seeding, cells were cultured in serum-free DMEM for 1 hour. Ten nanogram per milliliter of recombinant human TGF-β1 (R&D systems) was diluted in serum-free DMEM (1195-045; Gibco), and cells were treated for 24 hours. Changes in versican expression after stimulation were measured by real-time quantitative polymerase chain reaction (PCR) using a TaqMan assay for the corresponding human target. The Major Resources Table is given in the online-only Data Supplement.

Quantitative Real-Time PCR

RNA extraction was performed using the miRNeasy Mini Kit (Qiagen) following the manufacturers' protocol. RNA concentration (absorbance at 260 nm) and purity (260/280 nm ratio) were measured in 1 μL of eluted RNA using spectrophotometry (NanoDrop ND-1000; Thermo Scientific). RNA integrity was evaluated using the Agilent Bioanalyzer System and considered acceptable if the RNA integrity number was >7. The RNA was then reverse-transcribed using random hexamers with SuperScript VILO MasterMix (Invitrogen) according to manufacturers' protocol, with sample preparation being performed on a StarChill PCR rack to maintain low temperature. The reverse transcription product was diluted 1:15 to 1:25 using RNase-free water. TaqMan hydrolysis assays were used for quantitative PCR analysis. Data were analyzed using ViiA 7 software (Applied Biosystems). A minimum of 2 reference genes was used throughout the study, and stability of RNA isolation, reverse transcription, and quantitative PCR was determined by variability of and correlation between reference genes. Analysis of stability was also performed using geNorm, a commonly used algorithm for validation of reference gene stability based on the comparative cycle-to-threshold method.[19] Relative amounts of the targets were calculated using the $2^{-\Delta\Delta Cq}$ method,[20] with statistical analysis performed on ΔCq values.

Immunofluorescence Staining in Murine AsAo

Murine aortas were fixed for 24 hours in 4% formaldehyde at 4°C. In brief, 3-μm sections were deparaffinized in xylene and rehydrated in graded ethanol. The slides were unmasked using hot sodium citrate buffer (pH 6.0), then permeabilized for 20 minutes in 0.1% Triton X-100. Sections were blocked with 10% serum at room temperature, before incubation with primary antibodies against LRP1 and α–smooth muscle actin or species-matched isotopes overnight at 4°C. After washes in PBS with 0.1% Tween 20, sections were incubated for 1 hour at room temperature with the secondary antibody. Nuclei were stained using DAPI for 10 minutes. Sections were visualized under a Nikon spinning disk confocal microscope, and images were acquired using NIS-elements 4.0 software. Scale bars are included in the images as indicated in the figure legends.

Transfection Experiments in Human Aortic SMCs

Human aortic SMCs were purchased from Lonza and cultured in SMC medium (cc-3183; Lonza) with 5% fetal bovine serum (Lonza). SMCs were seeded into 6-well tissue culture plates, and 24 hours after seeding, cells were transfected with 50 nmol/L of *LRP1* siRNA (Dharmacon, M-004721-01-0005, targeted sequences: GCAAGAAGCCGGAGCAUGA, GAACAAACACACUGGCUAA, GCUAUGAGUUUAAGAAGUU, GCGCAUCGAUCUUCACAAA) using lipofectamine 2000 (Thermo Fisher Scientific) according to the manufacturer's instructions. Nontargeting siRNA served as control (Dharmacon, D-001206-14-05, targeted sequences: UAAGGCUAUGAAGAGAUAC, AUGUAUUGGCCUGUAUUAG, AUGAACGUGAAUUGCUCAA, UGGUUUACAUGUCGACUAA). Cells were incubated for 6 hours in Opti-MEM (11058-021; Gibco) with lipofectamine and siRNAs. After removal of transfection medium, SMCs were incubated with SMC medium with 5% fetal bovine serum for 48 hours. Then, cells were cultured in serum-free SMC medium for 24 hours. Medium was collected for protein measurements. Cells were harvested for quantitative PCR and Western blot analyses. Major Resources Table is given in the online-only Data Supplement. Four

milliliters of conditioned media were concentrated using 0.5 mL columns with 3 kDa filter (Amicon Ultra Centrifugal Filter Device; 3 KD). Five hundred milliliters of samples were added each time and centrifuged at $14\,000g$ for 40 minutes at 4°C until the residual volume was around 30 μL. Samples were then washed twice using 500 μL of 0.1% SDS each time. Protein concentrates were then used for Western blots. After conditioned medium collection, cell layers were washed 3× with cold phosphate-buffered saline to remove the residual medium. Cells were scraped off in cold phosphate-buffered saline and centrifugated for 1 minute at $15\,000g$. One hundred milliliters of 1× lysis buffer with 1:100 proteinase inhibitors and 25 mmol/L of EDTA were added to cell pellets. After resuspension, lysed cell pellets were vortexed and incubated for 20 minutes on ice. Protein concentration was measured using Pierce BCA Protein Assay Kit before Western blot analyses.

Immunofluorescence Staining in Human Aortic Specimen

Human aortic tissues were collected from patients undergoing AsAo replacement surgery at St. George's Hospital according to the local Research Ethics Committee (London, REC No. 08/H0803/257). Aortic tissues were fixed in 10% formalin and then embedded with paraffin. For antigen retrieval, chondroitinase ABC was applied on 5 μm tissue sections for 2 hours at 37°C. After blocking with 10% fetal bovine serum for 1 hour, sections were coincubated with primary antibodies against full-length versican and versican neoepitope DPEAAE[441] overnight at 4°C. Species-matched isotype IgGs were used as negative controls. After washes in PBS with 0.1% Tween 20, the appropriate secondary antibody was used for 1 hour at room temperature. Nuclei were stained with DAPI (1:1000 dilution) for 10 minutes. The images were visualized with an inverted Nikon Spinning disc confocal unit and acquired using NIS-elements 4.0 software.

Statistical Analysis

GraphPad Prism software 7 was used for the analysis. For each experiment, Shapiro–Wilk normality test was applied to test the distribution of the data. If the data were not normally distributed, a nonparametric test was used. The appropriate tests and post hoc analysis were chosen according to the data distribution as specified in each figure legend. Data are represented as mean±SD. For proteomics, statistical analysis was not performed if a protein was undetectable in the majority of samples from both groups compared. This is denoted as not applicable. Data from discovery proteomics are presented as normalized total ion current. Data obtained from targeted proteomics are presented as peak area and adjusted according to the total ion intensity for each sample. The aortic diameters are represented as box-and-whisker plots, with 75th and 25th percentiles; bars represent maximum and minimum values. Differences were assessed using a 2-way ANOVA and Šidák post hoc test. For all statistical analysis, $P<0.05$ was deemed significant.

Results

ADAMTS Expression in the Murine Aorta

Transcript levels of *Adamts5* were higher in the aortic arch compared with the other aortic regions, along with transcript levels of the large aggregating proteoglycans versican (*Vcan*) and aggrecan (*Acan*), 2 ADAMTS-5 substrates, which were most highly expressed in the arch. Expression of *Tgfb1* and *Tgfb2* and the receptors *Tgfbr2* and *Tgfbr3* were also higher in the arch compared with the abdominal aorta. In contrast, *Adamts1* and *Adamts4* and hyaluronan and proteoglycan link protein 1 (*Hapln1*) showed lower transcript levels in the arch compared with other regions of the murine aorta (Figure 1).

Aortic Dilatation in Adamts5^Δcat Mice

Loss of ADAMTS-1 has recently been implicated in TAA.[3] Thus, we assessed aortic dilatation in mice lacking the region
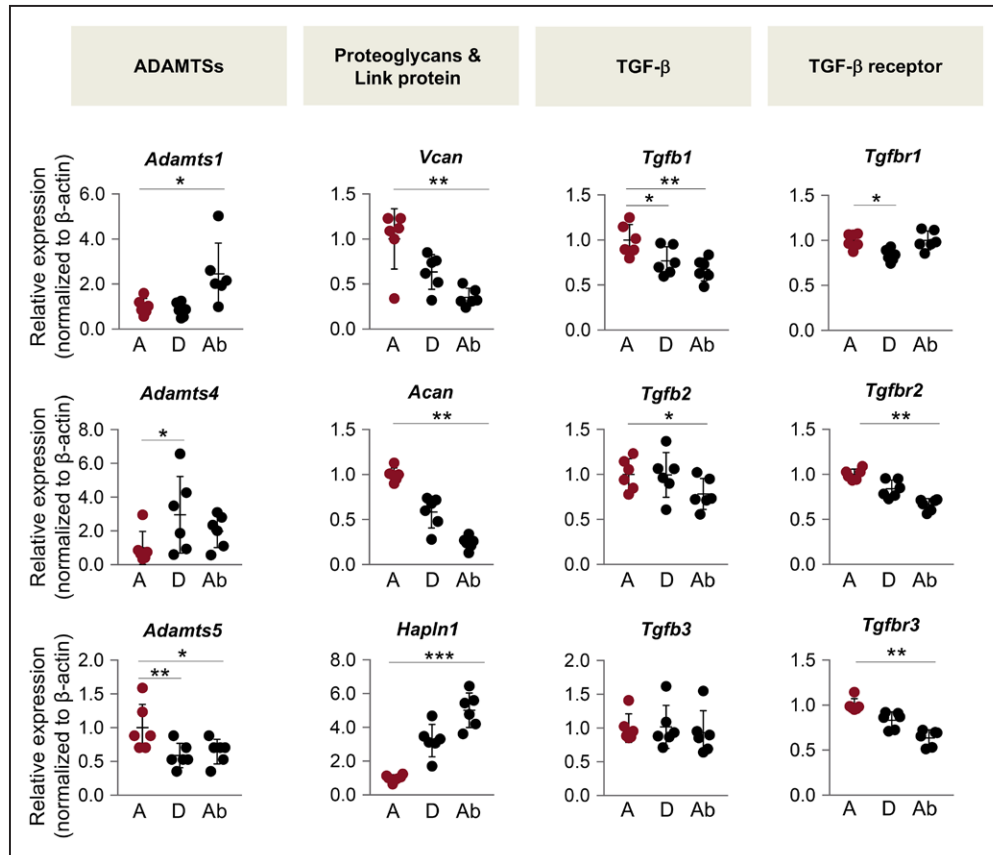
Figure 1. Gene expression along the murine aorta. Relative gene expression of *Adamts1* (a disintegrin and metalloproteinase with thrombospondin motifs 1), *Adamts4* and *Adamts5*, versican (*Vcan*), aggrecan (*Acan*) and hyaluronan and proteoglycan link protein 1 (*Hapln1*), and *Tgfb1* (transforming growth factor-β1), *Tgfb2* and *Tgfb3* and *Tgbr1* (transforming growth factor-β receptor type 1), *Tgbr2* and *Tgbr3* in the aortic arch (A), descending (D) and abdominal (Ab) aorta (n=6). β-actin was used as reference gene. Gene expression levels in the arch served as reference. Values are given as mean±SD; *P<0.05, **P<0.01, ***P<0.001 by Friedman test with Dunn post hoc comparison.

encoding for the catalytic domain of Adamts5 (Adamts5$^{\Delta cat}$).[21] Hypertension was induced in Adamts5$^{+/+}$ and Adamts5$^{\Delta cat}$ mice by AngII infusion for 4 weeks (Figure I in the online-only Data Supplement). AngII treatment was associated with increased aortic dilatation in Adamts5$^{\Delta cat}$ mice (Figure 2A and 2B); significant differences compared with Adamts5$^{+/+}$ were observed both in the aortic root, in particular in the aortic annulus, and the AsAo. Notably, the increased aortic dilatation in Adamts5$^{\Delta cat}$ mice occurred despite an attenuated rise in systolic and diastolic blood pressure after 27 days of AngII treatment (Figure 2C). The aortic phenotype and the blood pressure changes in Adamts5$^{\Delta cat}$ mice bear a strong resemblance to the one recently described in mice with Adamts1 haploinsufficiency.[3]

Vascular Substrates of ADAMTS-1 and ADAMTS-5
To identify vascular substrates of ADAMTS-1 and ADAMTS-5, murine aortas were subjected to overnight incubation with either ADAMTS-1 or ADAMTS-5 (50 pmol L^{-1} mg^{-1} tissue at 37°C; Figure 3A). Aortas incubated in buffer only served as control. The proteins released into the digestion buffer were separated by SDS-PAGE, subjected to in-gel tryptic digestion, and analyzed by liquid chromatography-tandem mass spectrometry. Among the identified extracellular proteins, proteins with differential release on digestion

by ADAMTS-1 and -5 include known substrates such as CSPG2 (versican; Figure 3B; Table I in the online-only Data Supplement). Detailed examination of the gel-liquid chromatography-tandem mass spectrometry data revealed the presence of proteolytic products (Figure 3C), that is, for CSPG2, CO6A6 (collagen type VI α-6), FINC (fibronectin), and LRP1. However, proteolytic cleavage may occur without differential release into the digestion buffer, that is, a higher number of MS/MS spectra for PGS1 (biglycan) and COCA1 (collagen type XII α-1) were identified in gel segments below the expected molecular weight of the full-length protein, indicative of proteolysis. Again, this includes known substrates of ADAMTS-5, such as PGS1.[22]

Proteomics Analysis of Aortas From AngII-Treated Wild-Type and Adamts5$^{\Delta cat}$ Mice
To analyze the changes in ECM composition on loss of ADAMTS-5 activity, aortas from AngII-treated Adamts5$^{+/+}$ and Adamts5$^{\Delta cat}$ mice were subjected to a 3-step sequential extraction procedure: pretreatment with 0.5 mol/L NaCl followed by decellularization with 0.08% SDS and a final incubation step with 4 mol/L GuHCl to solubilize the ECM (Figure 4A). Using a discovery proteomics approach, along with MFAP5 (microfibrillar-associated protein 5), CSPG2
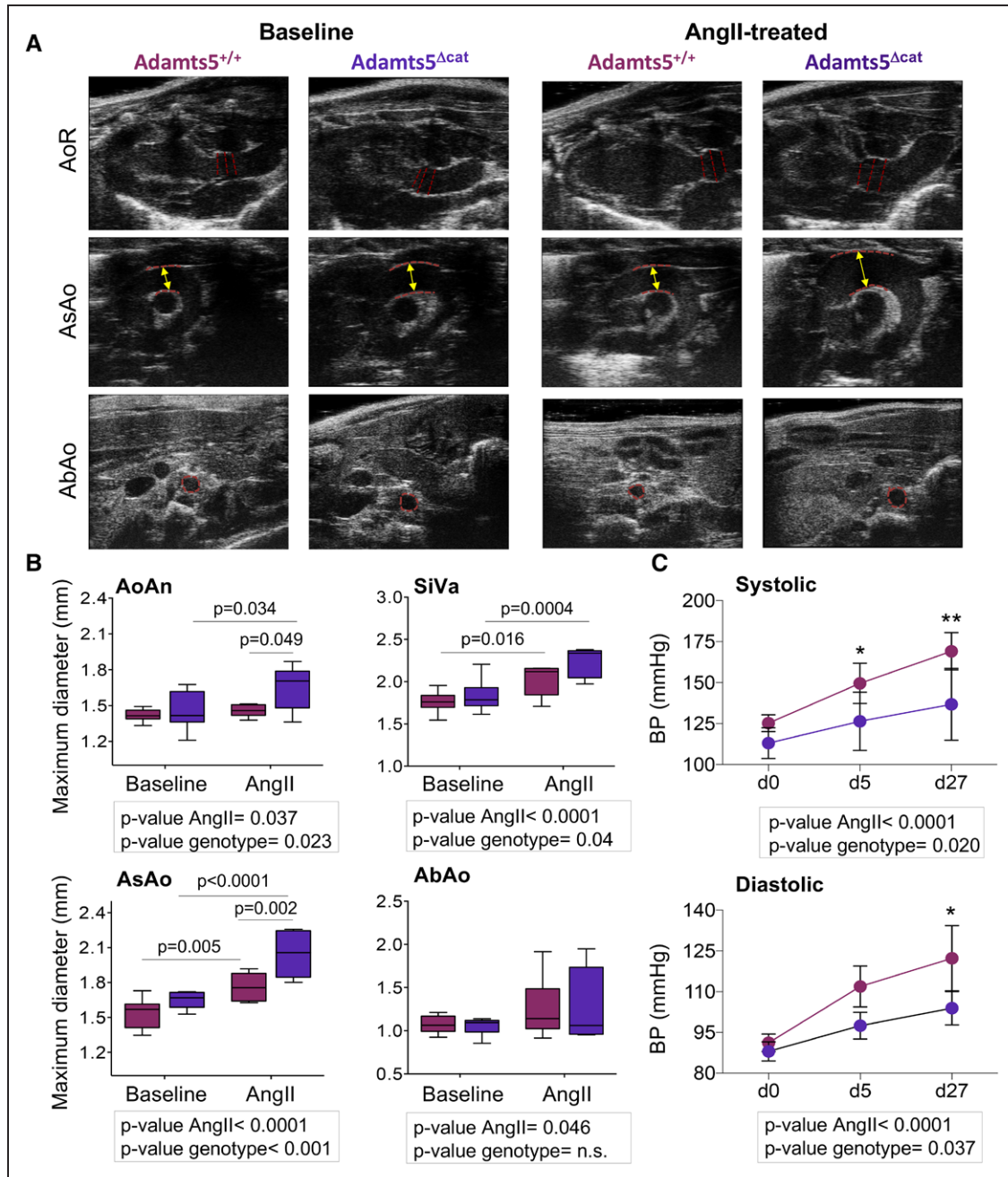
Figure 2. Aortic dilatation in mice lacking the region of the catalytic domain of a disintegrin and metalloproteinase with thrombospondin motifs-5 (Adamts5$^{\Delta cat}$ mice). **A**, Representative ultrasound images. Red dashed lines mark areas considered for aortic diameter measurements. **B**, Maximal diameters of the aortic ring (AoR; aortic annulus [AoAn] and sinuses of Valsalva [SiVa]), ascending aorta (AsAo), and abdominal aorta (AbAo) from AngII (angiotensin II)-treated (Adamts5$^{+/+}$, n=6 and Adamts5$^{\Delta cat}$, n=5) and untreated (Adamts5$^{+/+}$, n=9 and Adamts5$^{\Delta cat}$, n=9) mice. Adamts5$^{+/+}$ and Adamts5$^{\Delta cat}$ mice are represented using burgundy and purple color, respectively. **C**, Systolic and diastolic blood pressure (BP) measurements at day 0, 5, and after 27 days of AngII infusion in Adamts5$^{+/+}$ (n=6) and Adamts5$^{\Delta cat}$ mice (n=4). Data points are mean±SD; *P* values were derived from a 2-way ANOVA (aortic diameter) and 1-way ANOVA (blood pressure) with Šidák correction. *$P<0.05$, **$P<0.01$.

was returned as more abundant in aortas of AngII-treated Adamts5$^{\Delta cat}$ mice (Figure 4B; Table II in the online-only Data Supplement). Subsequent targeted proteomics analysis using both N-terminal and C-terminal proteotypic peptides corroborated that versican was elevated in AngII-treated Adamts5$^{\Delta cat}$ mice (Figure 4C; Table III in the online-only Data Supplement). TGF-β1 is known to enhance versican expression.[23] Human arterial SMCs stimulated with TGF-β1 showed a rise in versican transcripts (Figure 4D). Notably, higher levels of versican

were associated with increased protein abundance of TGF-β in aortas of AngII-treated Adamts5$^{\Delta cat}$ mice (Figure 4E; Figure II in the online-only Data Supplement). Gene expression levels of *Tgfb1 and 2* and their receptors *Tgfbr1-3* were significantly higher in Adamts5$^{\Delta cat}$ mice at baseline (Figure III in the online-only Data Supplement). Interestingly, *Adamts1* transcripts were markedly elevated in Adamts5$^{\Delta cat}$ mice, suggesting a compensatory increase of ADAMTS-1 on loss of ADAMTS-5 activity.
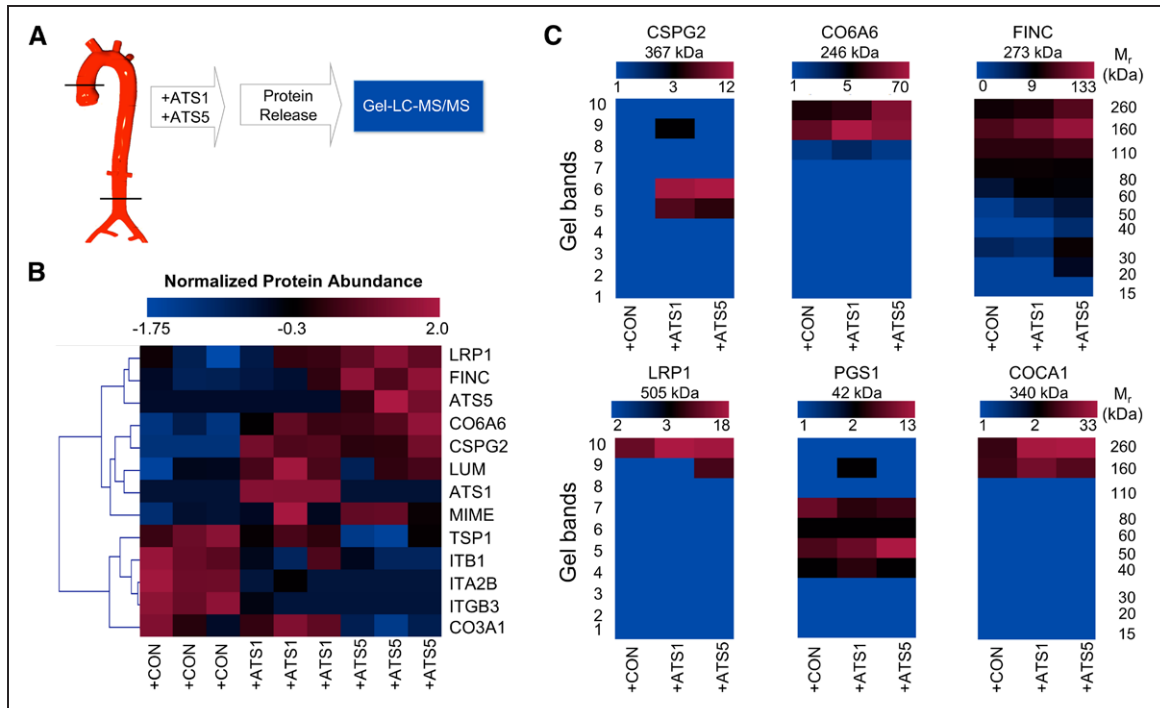
Figure 3. Proteomics to identify vascular targets of ADAMTS (a disintegrin and metalloproteinase with thrombospondin motifs)-1 and -5. **A**, Murine aortas were subjected to overnight incubation with either 50 pmol/L ADAMTS-1 (+ATS1) or 50 pmol/L ADAMTS-5 (+ATS5) at 37°C. Aortic explants incubated in buffer served as control (+CON). **B**, Unsupervised hierarchical clustering of the differentially released ECM (extracellular matrix) proteins (55 proteins were tested by Kruskal–Willis test, and 13 were found differentially regulated; *P*<0.05) in the supernatants of mouse aortas as identified by proteomics (n=3). The blue–red heat map represents normalized spectral counts highlighting differences in proteins released from aortic explants. **C**, Spectral evidence for fragmentation. The color-coded heat map represents the total number of identified spectra in each gel band and visualizes the fragmentation of ECM proteins. Color scales for heat maps represent maximum and minimum number of spectra identified in each group. COCA1 indicates collagen type XII α1 chain; CO6A6, collagen type VI α6 chain; CSPG2, versican; FINC, fibronectin; LC-MS/MS, liquid chromatography-tandem mass spectrometry; LRP1, low-density lipoprotein receptor-related protein 1; and PGS1, biglycan.

Versican Cleavage in Aortas of Adamts5Δcat Mice

Versican was the most differentially regulated ECM protein in aortas from Adamts5Δcat mice treated with AngII (Figure 4B). It was also returned as one of the major substrates of ADAMTS-1 and -5 in the analysis of aortic explants (Figure 3B). Therefore, we focused on ADAMTS-mediated versican processing. ADAMTS activity results in the release of a specific versican fragment ending with the DPEAAE441 sequence,[11,24] named versikine.[25] This signature cleavage site of ADAMTS activity can be detected using a neoepitope antibody (Figure 5A). As expected, aortas from Adamts5Δcat mice displayed reduced versikine; the 65 kDa band is representative of versikine (Figure 5B). Even after AngII treatment, less versikine was observed in Adamts5Δcat mice. This highlights the dependence on ADAMTS-5 activity for versicanolysis in AngII-induced aortic remodeling (Figure 5C).

Compensatory Increase of ADAMTS-1 in Aortas of Adamts5Δcat Mice

Because of different processing, ADAMTS-1 can be found in 2 forms, a larger, cell layer and ECM-associated version, and a smaller, soluble version (Figure 5A).[26] Immunoblotting for ADAMTS-1 performed on total aortic tissue lysates revealed that the loss of ADAMTS-5 activity was accompanied by an increase in the smaller, soluble form of ADAMTS-1 (65 kDa). This was exacerbated after AngII treatment. In contrast, the larger, ECM-associated ADAMTS-1 form (79 kDa)

was detected almost exclusively in the wild-type group. The increase in soluble ADAMTS-1 suggests a cross-talk between members of the ADAMTS protease family; however, this compensatory upregulation did not result in the complete rescue of ADAMTS-mediated versican cleavage (Figure 5C).

Reduced LRP1 in AngII-Treated Aortas of Adamts5Δcat Mice

To further investigate the molecular mechanisms associated with the loss of ADAMTS-5 activity, we analyzed LRP1, a receptor implicated in the endocytosis of ADAMTS proteases. LRP1 was identified as a vascular target of ADAMTS-1 and -5 (Figure 3). LRP1 was profoundly reduced in aortas of AngII-treated Adamts5Δcat mice (Figure 5C; Figure IV in the online-only Data Supplement). LRP1 staining was mainly observed in SMCs of mouse aortas (Figure 6A). Next, we silenced *LRP1* expression in primary human aortic SMCs. Silencing LRP1 did not affect *ADAMTS1* gene expression but markedly reduced expression of *ADAMTS5* (Figure 6B). Consequently, versikine was barely detectable in the conditioned media of SMCs transfected with an siRNA to *LRP1* (Figure 6C; Figure V in the online-only Data Supplement). Moreover, in agreement with our results in AngII-treated Adamts5Δcat mice, we observed a concomitant increase in ADAMTS-1 on repression of LRP1. Thus, these in vitro experiments complement our in vivo findings and establish a link between LRP1 and ADAMTS-5–mediated versican cleavage.
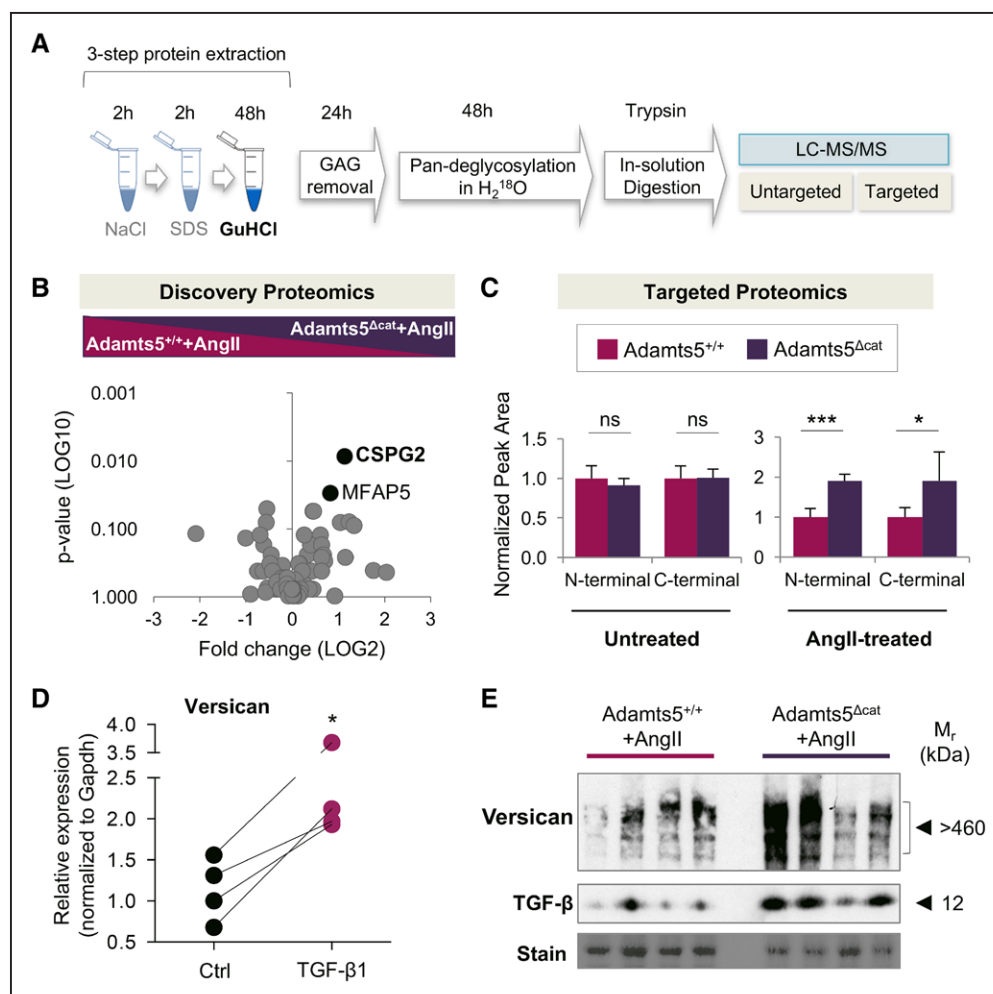
Figure 4. ECM (extracellular matrix) proteomics of AngII (angiotensin II)-treated murine aortas. **A**, ECM proteomics workflow. **B**, ECM extracts of the entire aorta from AngII-treated Adamts5^{+/+} (a disintegrin and metalloproteinase with thrombospondin motifs; n=6) and Adamts5[Δcat] (n=5) mice were analyzed using discovery proteomics. Black dots represent proteins differentially regulated between the groups (P<0.05). Statistical significance was calculated using Mann–Whitney test (76 ECM and ECM-associated proteins were tested, and 2 were found differentially regulated). **C**, Two different proteotypic peptides (ie, N-terminal and C-terminal) were chosen to validate levels of versican in aortic tissue using targeted proteomics. Peak area values of versican in Adamts5^{+/+} served as reference for N-terminal and C-terminal peptides. Statistical significance was calculated using unpaired Student t test. **D**, Internal mammary artery smooth muscle cells (SMCs) from 4 donors were incubated with TGF (transforming growth factor)-β1. Gene expression of versican was assessed by quantitative PCR. Gapdh was used as internal control. Statistical significance was calculated using unpaired Student t test. **E**, Immunoblots performed on total protein lysates reveal an increase in full-length versican and TGF-β in aortas of AngII-treated Adamts5[Δcat] mice (n=4 per group). CSPG2 denotes versican; GAG, glycosaminoglycan; GuHCl, guanidine hydrochloride; LC-MS/MS, liquid chromatography-tandem mass spectrometry; MFAP5, microfibrillar-associated protein 5; and n.s., not significant.

Versican Cleavage in Human Aortic Aneurysms

Although differences in versican abundance have been reported in human abdominal aortic aneurysms,[27] versikine has not been localized yet in human AsAo aneurysms. Immunofluorescence staining was performed for versican and versikine. Versican staining was seen throughout the aortic wall, whereas versikine was localized predominantly in the outer media and the subintimal layer of the AsAo aneurysm (Figure 6D). These data confirm the presence of ADAMTS-specific versican cleavage in human ascending TAA tissue.

Discussion

We have characterized regional differences in ADAMTS expression along the murine aorta and used proteomics to evaluate the effect of loss of ADAMTS-5 activity on aortic ECM

remodeling. We demonstrated that deficiency of ADAMTS-5 affects ADAMTS-1 gene expression, protein abundance and processing and resulted in aortic dilatation similar to the phenotype recently described in Adamts1-haploinsufficient mice.[3]

ADAMTS Proteases in Murine Aortas

We have previously demonstrated that ADAMTS-5 is the most potent protease associated with versican cleavage in the murine aorta.[11] Loss of ADAMTS-5 also results in the accumulation of aggrecan.[12] To investigate the contribution of ADAMTS-5 in ECM remodeling during aortic aneurysm formation, a mouse model lacking ADAMTS-5 activity was used. Administration of AngII for 4 weeks exacerbated aortic dilatation in Adamts5[Δcat] mice, with a significantly greater diameter in the AsAo where *Adamts5* expression is the highest in Adamts5^{+/+}
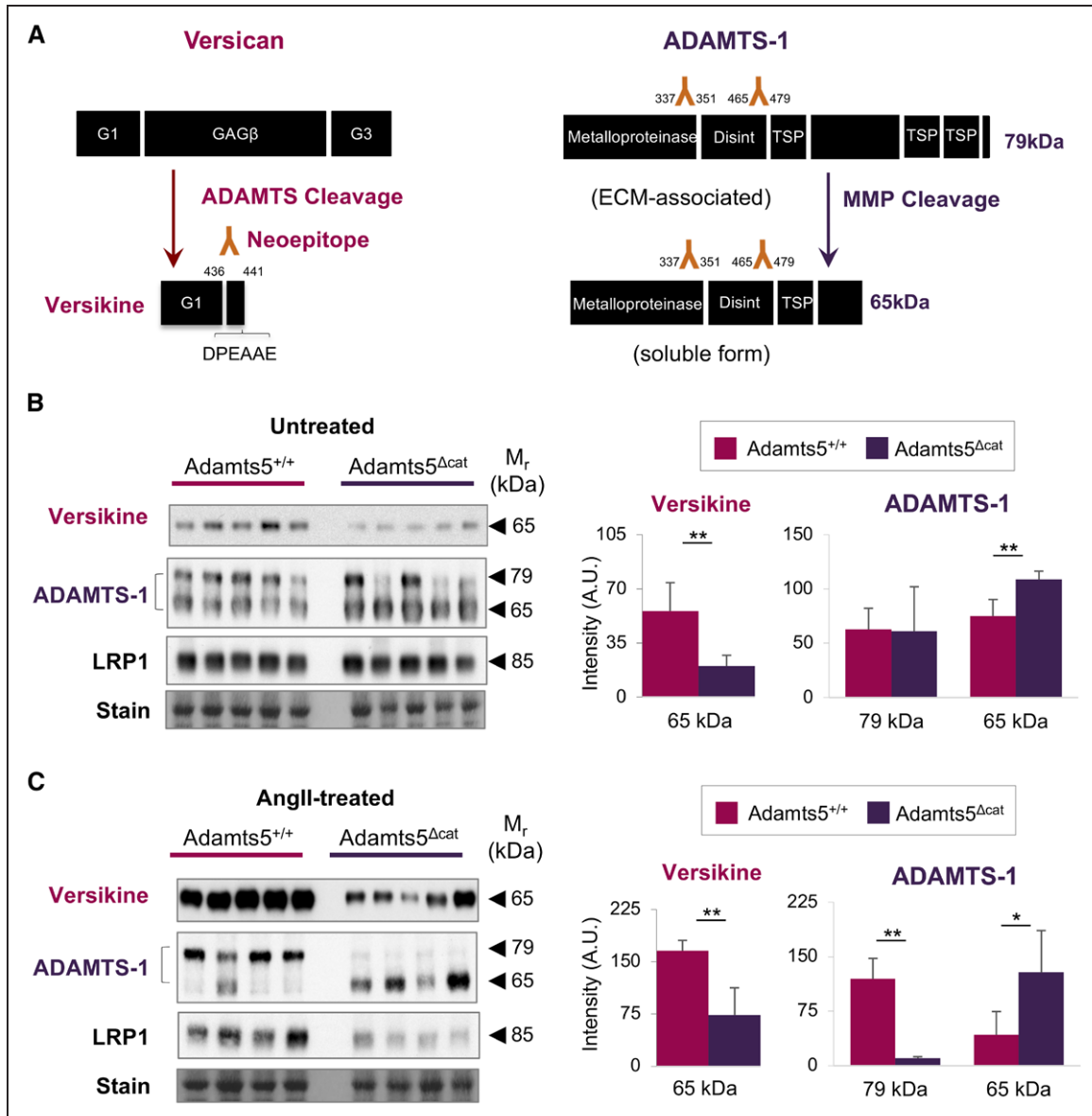
Figure 5. ADAMTS (a disintegrin and metalloproteinase with thrombospondin motifs)-1 cannot compensate for the lack of ADAMTS-5 activity. **A, Left,** Schematic representation of ADAMTS-mediated versican processing. The signature cleavage site for ADAMTS activity gives rise to an N-terminal versican fragment (versikine) and is recognized by a neoepitope antibody to the DPEAAE[441] amino acid sequence. **Right,** Schematic representation of ADAMTS-1 processing. Processing by MMPs (matrix metalloproteinases) gives rise to a truncated, soluble form of ADAMTS-1 (65 kDa). **B, C,** Immunoblots using neoepitope antibodies to versikine were performed on aortic ECM (extracellular matrix) extracts from untreated and AngII (angiotensin II)–treated mice (n=5 per group). Immunoblots for ADAMTS-1 and LRP1 (low-density lipoprotein-related protein 1) were performed on total protein lysates of untreated and AngII-treated mice (n=5 and n=4 per group, respectively). Densitometry for the versican fragment (versikine) and ADAMTS-1. Bars represent mean±SD. Statistical significance was calculated using unpaired Student *t* tests. *$P<0.05$, **$P<0.01$. A.U. indicates arbitrary unit; and TSP, trombospondin domain.

mice. Moreover, Adamts5[Δcat] mice showed an attenuated rise in blood pressure in response to AngII stimulation compared to Adamts5^{+/+} mice. Interestingly, a recent study reported a similar effect on blood pressure in Adamts1-haploinsufficient mice.[3] Also other ADAMTS proteases have been implicated in the vasculature and the regulation of blood pressure.[28]

Proteomics to Identify Vascular Substrates

In the current study, we used proteomics for the analysis of aortic ECM changes associated with loss of ADAMTS-5 activity. By using proteomics, we found that versican was more abundant in AngII-treated Adamts5[Δcat] mice. Versican is

one of the most abundant large aggregating proteoglycans in the aorta.[16] Tissue accumulation of versican has been linked to the loss of fibrous ECM organization.[29] Because we failed to detect changes in versican gene expression in Adamts5[Δcat] mice (data not shown), differences in versican protein abundance are most probably related to reduced degradation rather than protein synthesis. Versican is a well-known substrate of ADAMTS proteases.[30] Versican processing resulting in the release of versikine was also observed after incubation of human aortic tissues with either ADAMTS-1 or ADAMTS-5.[11] The absence of the catalytic activity of ADAMTS-5 seems to result in the build-up of unprocessed
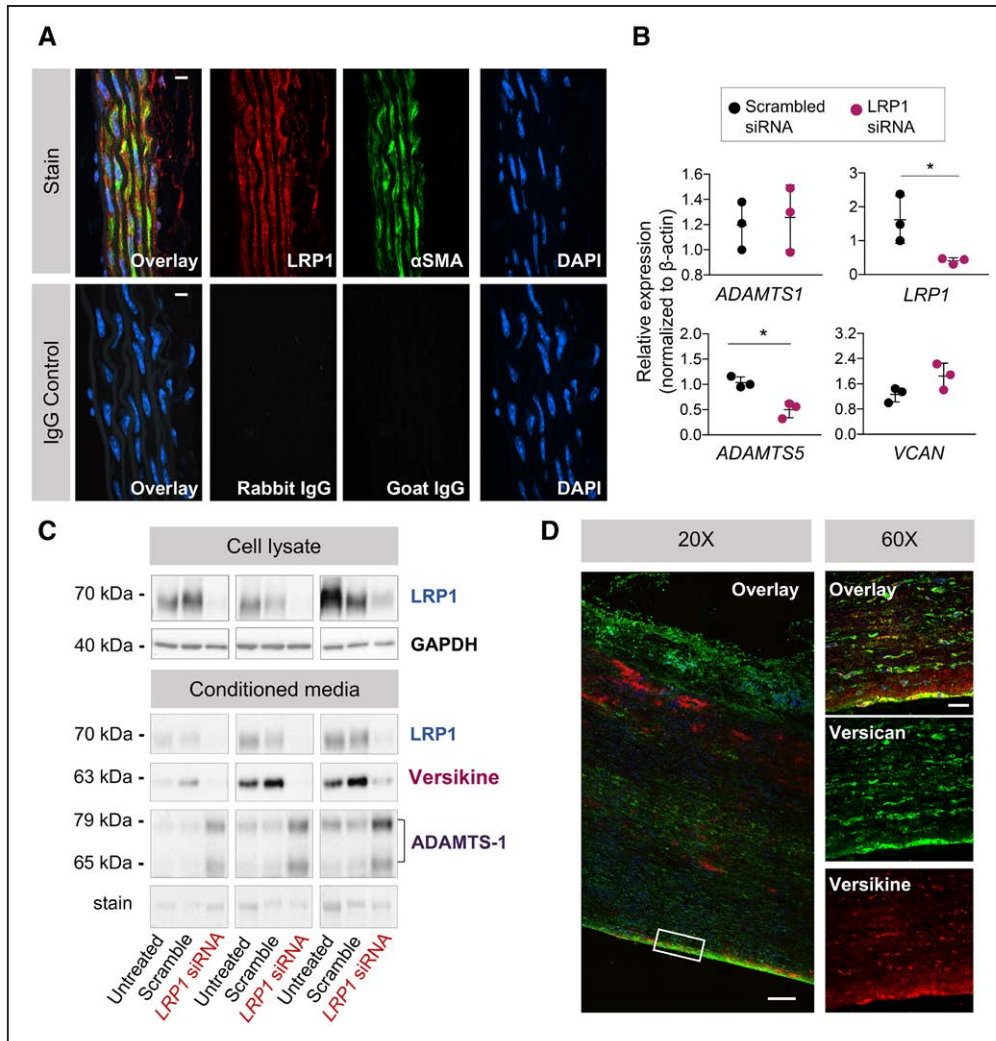
Figure 6. Effects of LRP1 (low-density lipoprotein-related protein 1) and detection of versikine in human ascending aortic aneurysms. **A**, LRP1 localization in the ascending aorta of mice lacking the catalytic domain of a disintegrin and metalloproteinase with thrombospondin motifs 5 (Adamts5$^{\Delta cat}$ mice). Colocalization of LRP1 (Alexa 647, displayed in red) and αSMA (alpha smooth muscle actin; Alexa 568, displayed in green) in the mouse aorta as visualized by immunofluorescence. Elastin fibers are in white (autofluorescence captured with 488 nm laser excitation). Control sections stained with isotope IgGs. Magnification ×60, scale bars=10 μm. **B**, Relative gene expression of *ADAMTS1*, *LRP1*, *ADAMTS5*, and *VCAN* in human aortic smooth muscle cells (SMCs) treated for 72 h with *LRP1* siRNA (n=3). β-actin was used as reference gene. Data points are mean±SD. Statistical significance was calculated using paired Student *t* tests. *$P<0.05$. **C**, Immunoblotting performed on cell lysate and conditioned media after transfection (n=3). Silencing LRP1 results in a decrease in versikine and an increase in ADAMTS-1 in the conditioned media. **D**, Localization of versican (Alexa568, displayed in green) and versikine (Alexa 647, displayed in red) in human ascending aortic aneurysms as visualized by immunofluorescence. Magnification ×20, scale bar=200 μm and ×60, scale bar=20 μm.

versican in the aortic wall, as previously observed in valve tissue of Adamts5$^{\Delta cat}$ mice.[13]

ADAMTS-Mediated Versicanolysis

Versican can be cleaved by different proteases including MMPs,[31] plasmin,[32] and several members of the ADAMTS family. The latter harbor sequence motifs specific to large aggregating proteoglycans, including versican. The neoepitope DPEAAE at position 441 of versican is generated after ADAMTS cleavage.[25] The neoepitope antibody recognizes only the cleaved product of versican, corresponding to the N-terminus of the proteoglycan.[25] This fragment was reduced in Adamts5$^{\Delta cat}$ mice, which is in agreement with our previous report.[11] As demonstrated in this study, this effect is exacerbated after AngII infusion; chronic infusion of AngII enhanced the release of versikine in murine aortas.

In AngII-treated Adamts5$^{\Delta cat}$ mice, immunoblotting revealed a marked reduction of the ADAMTS-specific DPEAAE neoepitope demonstrating the importance of ADAMTS-5 for versican cleavage. Versikine has been suggested to stimulate SMC migration and induce cell apoptosis during development.[33,34] Little residual ADAMTS activity was detectable in aortas of AngII-treated Adamts5$^{\Delta cat}$ mice. The latter is most likely attributable to ADAMTS-1, which was increased in Adamts5$^{\Delta cat}$ mice. ADAMTS-1 is known to be processed into 2 active forms: (1) an ECM-associated and (2) a soluble form, generated after MMP-mediated cleavage of the thrombospondin domain at the C-terminus. The loss of ADAMTS-5 activity led to a rise in the soluble form of ADAMTS-1, and this effect was exacerbated after AngII treatment. The removal of the last thrombospondin domain renders ADAMTS-1 more similar to ADAMTS-5, suggesting that the release of soluble

ADAMTS-1 could be a compensatory response to the loss of ADAMTS-5. ADAMTS-1, however, cannot sufficiently compensate for the lack of ADAMTS-5 activity, at least with regards to versican cleavage.

Effects on TGF-β

The increase in total versican levels was associated with a concomitant upregulation of TGF-β in Adamts5[Δcat] mice after AngII treatment. TGF-β is known to induce the expression of different proteoglycans, including versican.[23] In line with this finding, stimulation of arterial SMCs with TGF-β1 led to an increase in versican expression. Interestingly, it has also been shown that the latent form of TGF-β can be associated and subsequently activated by the C-terminal region of ADAMTS-1, thereby enhancing the inflammatory response in liver fibrosis.[35] In agreement with these results, we found a direct correlation between ADAMTS-1 and TGF-β regulation in ADAMTS-5[Δcat] mice on AngII treatment. Increased levels of versican, TGF-β, and ADAMTS-1 were accompanied by an increased aortic dilatation in these mice after AngII treatment. Dysregulation of TGF-β has been linked to aneurysm development.[36,37] However, the mechanisms of TGF-β–mediated aneurysm formation have not been completely elucidated yet. The present study highlights an effect of ADAMTS activity on TGF-β bioavailability.

Regulation by LRP1

LRP1 has previously been implicated in aortic aneurysm formation in humans and mice[14,38,39]; however, the exact mechanisms are unclear. LRP1 is involved in different cellular processes, such as lipid homeostasis, signal transduction, and endocytosis.[40,41] LRP1 also acts as a protease sink responsible for cellular uptake of ADAMTS-5 from the extracellular space.[42] Moreover, LRP1 can bind TGF-β1 and TGF-β2 and thereby inhibit cell proliferation and regulate vascular remodeling, respectively.[43] After AngII treatment, LRP1 was less abundant in aortas of Adamts5[Δcat] mice. This was accompanied by an increase in the short soluble form of ADAMTS-1 as a possible mechanism to compensate for the lack of ADAMTS-5. This coordinated regulation is consistent with a feedback mechanism between ADAMTS-5 and LRP1. A compensatory downregulation of LRP1 in AngII-treated Adamts5[Δcat] mice could increase the extracellular availability of other ADAMTS proteases. Silencing LRP1 in human aortic SMCs reduced *ADAMTS5* expression and resulted in a loss of ADAMTS-mediated versican cleavage. Again, this was accompanied by an increase of ADAMTS-1 in the conditioned media. These findings expand on a previous report that the deletion of *Lrp1* in SMCs augmented AsAo dilatation in AngII-treated mice.[14]

Limitations of the Study

A mouse model of AngII infusion was used to study the effects of ADAMTS-5 on aortic dilatation, which may not recapitulate all aspects of human aneurysmal disease, in particular with regards to hemodynamics and mechanotransduction.[44,45] Also, the relative importance of different members of the ADAMTS family may differ between species. In human

aneurysmal disease, previous studies have shown increased protein and transcript levels of ADAMTS-1 and -4 in TAA.[10] Consistent with our findings, a recent study reported decreased *ADAMTS5* expression and increased deposition of proteoglycans, such as aggrecan and versican in human TAA.[8] Finally, changes in ADAMTS activity are likely to be associated with the proteolysis of other proteins apart from versican.

Conclusions

At present, the clinical management of aneurysms is hampered by our limited knowledge about the cause and pathogenic mechanisms involved in the disease.[46] Evidence is emerging that ECM processing by members of the ADAMTS protease family could play an important role in the progression of aortic dilatation.[3] The present study takes advantage of proteomics to define vascular substrates of ADAMTS proteases. LRP1, which has been involved in aneurysm pathology in both humans and mice, appears to be linked to ADAMTS-5 and ADAMTS-5–mediated versican cleavage. In mice lacking ADAMTS-5 activity, AngII infusion results in decreased versicanolysis, an increase in full-length versican and TGF-β, but reduced LRP1 compared with wild-type controls. Mice lacking ADAMTS-5 activity also showed increased aortic dilatation in response to AngII infusion despite a lower blood pressure. A compensatory rise in ADAMTS-1 could not prevent aortic dilatation in Adamts5[Δcat] mice, suggesting a greater contribution of ADAMTS-5 in this context. Further studies are needed to explore the ADAMTS protease family as a therapeutic target to reduce or halt dilatation of the aorta resulting in dissection.

Disclosures

None.

References

1. Bonderman D, Gharehbaghi-Schnell E, Wollenek G, Maurer G, Baumgartner H, Lang IM. Mechanisms underlying aortic dilatation in congenital aortic valve malformation. *Circulation*. 1999;99:2138–2143.
2. He R, Guo DC, Sun W, Papke CL, Duraisamy S, Estrera AL, Safi HJ, Ahn C, Buja LM, Arnett FC, Zhang J, Geng YJ, Milewicz DM. Characterization

of the inflammatory cells in ascending thoracic aortic aneurysms in patients with Marfan syndrome, familial thoracic aortic aneurysms, and sporadic aneurysms. *J Thorac Cardiovasc Surg*. 2008;136:922, 929.e1–929, 929.e1. doi: 10.1016/j.jtcvs.2007.12.063.

3. Oller J, Méndez-Barbero N, Ruiz EJ, et al. Nitric oxide mediates aortic disease in mice deficient in the metalloprotease Adamts1 and in a mouse model of Marfan syndrome. *Nat Med*. 2017;23:200–212. doi: 10.1038/nm.4266.

4. Jones JA, Spinale FG, Ikonomidis JS. Transforming growth factor-beta signaling in thoracic aortic aneurysm development: a paradox in pathogenesis. *J Vasc Res*. 2009;46:119–137. doi: 10.1159/000151766.

5. Shen M, Lee J, Basu R, Sakamuri SS, Wang X, Fan D, Kassiri Z. Divergent roles of matrix metalloproteinase 2 in pathogenesis of thoracic aortic aneurysm. *Arterioscler Thromb Vasc Biol*. 2015;35:888–898. doi: 10.1161/ATVBAHA.114.305115.

6. Ikonomidis JS, Jones JA, Barbour JR, Stroud RE, Clark LL, Kaplan BS, Zeeshan A, Bavaria JE, Gorman JH III, Spinale FG, Gorman RC. Expression of matrix metalloproteinases and endogenous inhibitors within ascending aortic aneurysms of patients with bicuspid or tricuspid aortic valves. *J Thorac Cardiovasc Surg*. 2007;133:1028–1036. doi: 10.1016/j.jtcvs.2006.10.083.

7. Ren P, Hughes M, Krishnamoorthy S, Zou S, Zhang L, Wu D, Zhang C, Curci JA, Coselli JS, Milewicz DM, LeMaire SA, Shen YH. Critical role of ADAMTS-4 in the development of sporadic aortic aneurysm and dissection in mice. *Sci Rep*. 2017;7:12351. doi: 10.1038/s41598-017-12248-z.

8. Cikach FS, Koch CD, Mead TJ, Galatioto J, Willard BB, Emerton KB, Eagleton MJ, Blackstone EH, Ramirez F, Roselli EE, Apte SS. Massive aggrecan and versican accumulation in thoracic aortic aneurysm and dissection. *JCI Insight*. 2018;3:1–16. doi: 10.1172/jci.insight.97167.

9. Kenagy RD, Min SK, Clowes AW, Sandy JD. Cell death-associated ADAMTS4 and versican degradation in vascular tissue. *J Histochem Cytochem*. 2009;57:889–897. doi: 10.1369/jhc.2009.953901.

10. Ren P, Zhang L, Xu G, Palmero LC, Albini PT, Coselli JS, Shen YH, LeMaire SA. ADAMTS-1 and ADAMTS-4 levels are elevated in thoracic aortic aneurysms and dissections. *Ann Thorac Surg*. 2013;95:570–577. doi: 10.1016/j.athoracsur.2012.10.084.

11. Didangelos A, Mayr U, Monaco C, Mayr M. Novel role of ADAMTS-5 protein in proteoglycan turnover and lipoprotein retention in atherosclerosis. *J Biol Chem*. 2012;287:19341–19345. doi: 10.1074/jbc.C112.350785.

12. Suna G, Wojakowski W, Lynch M, et al. Extracellular matrix proteomics reveals interplay of aggrecan and aggrecanases in vascular remodeling of stented coronary arteries. *Circulation*. 2018;137:166–183. doi: 10.1161/CIRCULATIONAHA.116.023381.

13. Dupuis LE, McCulloch DR, McGarity JD, Bahan A, Wessels A, Weber D, Diminich AM, Nelson CM, Apte SS, Kern CB. Altered versican cleavage in ADAMTS5 deficient mice; a novel etiology of myxomatous valve disease. *Dev Biol*. 2011;357:152–164. doi: 10.1016/j.ydbio.2011.06.041.

14. Davis FM, Rateri DL, Balakrishnan A, Howatt DA, Strickland DK, Muratoglu SC, Haggerty CM, Fornwalt BK, Cassis LA, Daugherty A. Smooth muscle cell deletion of low-density lipoprotein receptor-related protein 1 augments angiotensin II-induced superior mesenteric arterial and ascending aortic aneurysms. *Arterioscler Thromb Vasc Biol*. 2015;35:155–162. doi: 10.1161/ATVBAHA.114.304683.

15. Barallobre-Barreiro J, Oklu R, Lynch M, Fava M, Baig F, Yin X, Barwari T, Potier DN, Albadawi H, Jahangiri M, Porter KE, Watkins MT, Misra S, Stoughton J, Mayr M. Extracellular matrix remodelling in response to venous hypertension: proteomics of human varicose veins. *Cardiovasc Res*. 2016;110:419–430. doi: 10.1093/cvr/cvw075.

16. Didangelos A, Yin X, Mandal K, Baumert M, Jahangiri M, Mayr M. Proteomics characterization of extracellular space components in the human aorta. *Mol Cell Proteomics*. 2010;9:2048–2062. doi: 10.1074/mcp.M110.001693.

17. Barallobre-Barreiro J, Didangelos A, Yin X, Doménech N, Mayr M. A sequential extraction methodology for cardiac extracellular matrix prior to proteomics analysis. *Methods Mol Biol*. 2013;1005:215–223. doi: 10.1007/978-1-62703-386-2_17.

18. Turner NA, Ho S, Warburton P, O'Regan DJ, Porter KE. Smooth muscle cells cultured from human saphenous vein exhibit increased proliferation, invasion, and mitogen-activated protein kinase activation in vitro compared with paired internal mammary artery cells. *J Vasc Surg*. 2007;45:1022–1028. doi: 10.1016/j.jvs.2007.01.061.

19. Vandesompele J, De Preter K, Pattyn F, Poppe B, Van Roy N, De Paepe A, Speleman F. Accurate normalization of real-time quantitative RT-PCR data by geometric averaging of multiple internal control genes. *Genome Biol*. 2002;3:1–12.

20. Livak KJ, Schmittgen TD. Analysis of relative gene expression data using real-time quantitative PCR and the 2(-Delta Delta C(T)) method. *Methods*. 2001;25:402–408. doi: 10.1006/meth.2001.1262.

21. Stanton H, Rogerson FM, East CJ, Golub SB, Lawlor KE, Meeker CT, Little CB, Last K, Farmer PJ, Campbell IK, Fourie AM, Fosang AJ. ADAMTS5 is the major aggrecanase in mouse cartilage in vivo and in vitro. *Nature*. 2005;434:648–652. doi: 10.1038/nature03417.

22. Melching LI, Fisher WD, Lee ER, Mort JS, Roughley PJ. The cleavage of biglycan by aggrecanases. *Osteoarthritis Cartilage*. 2006;14:1147–1154. doi: 10.1016/j.joca.2006.05.014.

23. Nikitovic D, Zafiropoulos A, Katonis P, Tsatsakis A, Theocharis AD, Karamanos NK, Tzanakakis GN. Transforming growth factor-beta as a key molecule triggering the expression of versican isoforms v0 and v1, hyaluronan synthase-2 and synthesis of hyaluronan in malignant osteosarcoma cells. *IUBMB Life*. 2006;58:47–53. doi: 10.1080/15216540500531713.

24. Sandy JD, Westling J, Kenagy RD, Iruela-Arispe ML, Verscharen C, Rodriguez-Mazaneque JC, Zimmermann DR, Lemire JM, Fischer JW, Wight TN, Clowes AW. Versican V1 proteolysis in human aorta in vivo occurs at the Glu441-Ala442 bond, a site that is cleaved by recombinant ADAMTS-1 and ADAMTS-4. *J Biol Chem*. 2001;276:13372–13378. doi: 10.1074/jbc.M009737200.

25. Nandadasa S, Foulcer S, Apte SS. The multiple, complex roles of versican and its proteolytic turnover by ADAMTS proteases during embryogenesis. *Matrix Biol*. 2014;35:34–41. doi: 10.1016/j.matbio.2014.01.005.

26. Rodriguez-Manzaneque JC, Milchanowski AB, Dufour EK, Leduc R, Iruela-Arispe ML. Characterization of METH-1/ADAMTS1 processing reveals two distinct active forms. *J Biol Chem*. 2000;275:33471–33479. doi: 10.1074/jbc.M002599200.

27. Theocharis AD, Tsolakis I, Hjerpe A, Karamanos NK. Human abdominal aortic aneurysm is characterized by decreased versican concentration and specific downregulation of versican isoform V(0). *Atherosclerosis*. 2001;154:367–376.

28. Gopalakrishnan K, Kumarasamy S, Abdul-Majeed S, Kalinoski AL, Morgan EE, Gohara AF, Nauli SM, Filipiak WE, Saunders TL, Joe B. Targeted disruption of Adamts16 gene in a rat genetic model of hypertension. *Proc Natl Acad Sci USA*. 2012;109:20555–20559. doi: 10.1073/pnas.1211290109.

29. Dupuis LE, Osinska H, Weinstein MB, Hinton RB, Kern CB. Insufficient versican cleavage and Smad2 phosphorylation results in bicuspid aortic and pulmonary valves. *J Mol Cell Cardiol*. 2013;60:50–59. doi: 10.1016/j.yjmcc.2013.03.010.

30. Foulcer SJ, Nelson CM, Quintero MV, Kuberan B, Larkin J, Dours-Zimmermann MT, Zimmermann DR, Apte SS. Determinants of versican-V1 proteoglycan processing by the metalloproteinase ADAMTS5. *J Biol Chem*. 2014;289:27859–27873. doi: 10.1074/jbc.M114.573287.

31. Halpert I, Sires UI, Roby JD, Potter-Perigo S, Wight TN, Shapiro SD, Welgus HG, Wickline SA, Parks WC. Matrilysin is expressed by lipid-laden macrophages at sites of potential rupture in atherosclerotic lesions and localizes to areas of versican deposition, a proteoglycan substrate for the enzyme. *Proc Natl Acad Sci USA*. 1996;93:9748–9753.

32. Kenagy RD, Fischer JW, Davies MG, Berceli SA, Hawkins SM, Wight TN, Clowes AW. Increased plasmin and serine proteinase activity during flow-induced intimal atrophy in baboon PTFE grafts. *Arterioscler Thromb Vasc Biol*. 2002;22:400–404.

33. Jönsson-Rylander AC, Nilsson T, Fritsche-Danielson R, Hammarström A, Behrendt M, Andersson JO, Lindgren K, Andersson AK, Wallbrandt P, Rosengren B, Brodin P, Thelin A, Westin A, Hurt-Camejo E, Lee-Søgaard CH. Role of ADAMTS-1 in atherosclerosis: remodeling of carotid artery, immunohistochemistry, and proteolysis of versican. *Arterioscler Thromb Vasc Biol*. 2005;25:180–185. doi: 10.1161/01.ATV.0000150045.27127.37.

34. McCulloch DR, Nelson CM, Dixon LJ, Silver DL, Wylie JD, Lindner V, Sasaki T, Cooley MA, Argraves WS, Apte SS. ADAMTS metalloproteases generate active versican fragments that regulate interdigital web regression. *Dev Cell*. 2009;17:687–698. doi: 10.1016/j.devcel.2009.09.008.

35. Bourd-Boittin K, Bonnier D, Leyme A, Mari B, Tuffery P, Samson M, Ezan F, Baffet G, Theret N. Protease profiling of liver fibrosis reveals the ADAM metallopeptidase with thrombospondin type 1 motif, 1 as a central activator of transforming growth factor beta. *Hepatology*. 2011;54:2173–2184. doi: 10.1002/hep.24598.

36. Chen X, Lu H, Rateri DL, Cassis LA, Daugherty A. Conundrum of angiotensin II and TGF-β interactions in aortic aneurysms. *Curr Opin Pharmacol*. 2013;13:180–185. doi: 10.1016/j.coph.2013.01.002.

37. Angelov SN, Hu JH, Wei H, Airhart N, Shi M, Dichek DA. TGF-β (Transforming Growth Factor-β) signaling protects the thoracic and abdominal aorta from angiotensin II-induced pathology by distinct

mechanisms. *Arterioscler Thromb Vasc Biol*. 2017;37:2102–2113. doi: 10.1161/ATVBAHA.117.309401.

38. Galora S, Saracini C, Pratesi G, Sticchi E, Pulli R, Pratesi C, Abbate R, Giusti B. Association of rs1466535 LRP1 but not rs3019885 SLC30A8 and rs6674171 TDRD10 gene polymorphisms with abdominal aortic aneurysm in Italian patients. *J Vasc Surg*. 2015;61:787–792. doi: 10.1016/j.jvs.2013.10.090.

39. Chan CY, Chan YC, Cheuk BL, Cheng SW. A pilot study on low-density lipoprotein receptor-related protein-1 in Chinese patients with abdominal aortic aneurysm. *Eur J Vasc Endovasc Surg*. 2013;46:549–556. doi: 10.1016/j.ejvs.2013.08.006.

40. Lillis AP, Muratoglu SC, Au DT, Migliorini M, Lee MJ, Fried SK, Mikhailenko I, Strickland DK. LDL Receptor-Related Protein-1 (LRP1) regulates cholesterol accumulation in macrophages. *PLoS One*. 2015;10:e0128903. doi: 10.1371/journal.pone.0128903.

41. Zurhove K, Nakajima C, Herz J, Bock HH, May P. Gamma-secretase limits the inflammatory response through the processing of LRP1. *Sci Signal*. 2008;1:ra15. doi: 10.1126/scisignal.1164263.

42. Yamamoto K, Troeberg L, Scilabra SD, Pelosi M, Murphy CL, Strickland DK, Nagase H. LRP-1-mediated endocytosis regulates extracellular

activity of ADAMTS-5 in articular cartilage. *FASEB J*. 2013;27:511–521. doi: 10.1096/fj.12-216671.

43. Strickland DK, Au DT, Cunfer P, Muratoglu SC. Low-density lipoprotein receptor-related protein-1: role in the regulation of vascular integrity. *Arterioscler Thromb Vasc Biol*. 2014;34:487–498. doi: 10.1161/ATVBAHA.113.301924.

44. Collins C, Osborne LD, Guilluy C, Chen Z, O'Brien ET III, Reader JS, Burridge K, Superfine R, Tzima E. Haemodynamic and extracellular matrix cues regulate the mechanical phenotype and stiffness of aortic endothelial cells. *Nat Commun*. 2014;5:3984. doi: 10.1038/ncomms4984.

45. Youssefi P, Gomez A, He T, Anderson L, Bunce N, Sharma R, Figueroa CA, Jahangiri M. Patient-specific computational fluid dynamics-assessment of aortic hemodynamics in a spectrum of aortic valve pathologies. *J Thorac Cardiovasc Surg*. 2017;153:8.e3–20.e3. doi: 10.1016/j.jtcvs.2016.09.040.

46. Didangelos A, Yin X, Mandal K, Saje A, Smith A, Xu Q, Jahangiri M, Mayr M. Extracellular matrix composition and remodeling in human abdominal aortic aneurysms: a proteomics approach. *Mol Cell Proteomics*. 2011;10:M111.008128. doi: 10.1074/mcp.M111.008128.

Highlights

- Expression of ADAMTS-5 (a disintegrin and metalloproteinase with thrombospondin motifs-5) and the large aggregating proteoglycans is higher in the aortic arch compared with the abdominal aorta.
- AngII (angiotensin II) treatment in Adamts5$^{\Delta cat}$ mice is associated with increased dilatation of the ascending aorta.
- Loss of ADAMTS-5 activity induces an accumulation of versican on AngII treatment.
- This is accompanied by an increase in TGF-β (transforming growth factor-β) levels and a compensatory upregulation of soluble ADAMTS-1.
- Silencing of LRP1 (low-density lipoprotein-related protein 1) in human aortic smooth muscle cells reduces ADAMTS-5 expression, attenuates ADAMTS-mediated versican cleavage, and increases ADAMTS-1.

Arteriosclerosis, Thrombosis, and Vascular Biology

American Heart Association

Role of ADAMTS-5 in Aortic Dilatation and Extracellular Matrix Remodeling

Marika Fava, Javier Barallobre-Barreiro, Ursula Mayr, Ruifang Lu, Athanasios Didangelos, Ferheen Baig, Marc Lynch, Norman Catibog, Abhishek Joshi, Temo Barwari, Xiaoke Yin, Marjan Jahangiri and Manuel Mayr

The online version of this article, along with updated information and services, is located on the
World Wide Web at:
http://atvb.ahajournals.org/content/38/7/1537
Free via Open Access

Data Supplement (unedited) at:
http://atvb.ahajournals.org/content/suppl/2018/04/03/ATVBAHA.117.310562.DC1

Major Resources Tables

Animals

Species/Strain	Vendor or Source	Background Strain	Sex
Wildtype mice	The Jackson Laboratory	C57BL/6J	male
Adamts5$^{\Delta cat}$	The Jackson Laboratory	129P2/OlaHs backcrossed 5 times onto C57BL/6J, one additional backcross was performed to generate the littermates for experiments	male

Primary Antibodies

Target antigen	Vendor or Source	Catalog #	Working concentration	Lot #
Neoepitope on versican generated by ADAMTS cleavage	Abcam	ab19345	WB: 1µg/ml IHC: 10µg/ml	GR314383-6
Full-length versican	Millipore	AB1033	WB: 0.5µg/ml	2867545
Full-length versican	Millipore	MABT161	IHC: 2.5µg/ml	2702191
ADAMTS-1	Thermo Fisher	720329	WB: 2µg/ml	SA246704
TGFß	Abcam	ab179695	WB: 0.512µg/ml	GR262076-2
LRP1	Abcam	ab92544	WB: 0.512µg/ml IHC: 4.6µg/ml	GR259330-25
GAPDH	Sigma	G8795	WB: 0.05µg/ml	056M-4856V
Alpha smooth muscle actin	Abcam	Ab21027	IHC:4µg/ml	GR309074-1

Secondary Antibodies

Vendor or Source	Target Species	Catalog #	Working concentration	Lot #
Jackson ImmunoResearch	Rabbit	211-032-171	WB: 80ng/ml	130846
Jackson ImmunoResearch	Mouse	115-035-174	WB: 80ng/ml	129518
Invitrogen	Rabbit	A21069	IHC: 2.5 µg/ml	1736974
Invitrogen	Mouse	A21203	IHC: 2.5 µg/ml	987237
Invitrogen	Rabbit	A31573	IHC: 2.5 µg/ml	1900251
Invitrogen	Goat	A11055	IHC: 2.5 µg/ml	1081957

Cultured Cells

Name	Vendor or Source	Sex (F, M, or unknown)
Human aortic SMCs	Lonza, US	Male
Human internal mammary artery SMCs	Dr. Karen Porter, Leeds Institute of Cardiovascular and Metabolic Medicine	Unknown

Material

Name	Company	Catalog Number
1.Chemicals		
Cocktail of proteinase inhibitor	Thermo Scientific	51101
Chloroform	Sigma-Aldrich	C2432
Phosho STOP	Roche	4906837001
Cell Lysis buffer	Cell Signalling	9803
NuPAGE MOPS SDS Running Buffer (20X)	Life Technologies	NP0001-02
EDTA	Sigma-Aldrich	E9884
EGTA	Sigma-Aldrich	E3889
Ethanol	VWR	437433T
Formalin	Sigma-Aldrich	HT501128
Guanidine hydrochloride	Sigma-Aldrich	G3272
$H_2^{18}O$	Taiyo Nippon Salso	FO3-0027
Iodoacetamine	Sigma-Aldrich	A3221
Glycine	Sigma-Aldrich	G8896

Lipofectamine 2000	Invitrogen	12566014
Methanol	Fisher Chemical	A4545K
Phosphate-buffered saline (PBS), 10X	Lonza	51226
Ponceau	Sigma-Aldrich	P7170
Quiazol Lysis Reagent	Qiagen	4053228006220
Sodium Acetate	Sigma-Aldrich	S7545
Sodium Azide	Sigma-Aldrich	08591
Sodium Chloride	Sigma-Aldrich	S9888
Sodium dedrcyl sulfate, SDS	Sigma-Aldrich	466143
Sodium Citrate dihydrate	Sigma-Aldrich	W302600
Super Script VILO MasterMix	Invitrogen	11755050
TaqMan Universal PCR Master Mix	Applied Biosystem	4324018
Triethylammonium bicarbonate (TEAB)	Sigma-Aldrich	11268
Trifluoroacetic acid (TFA)	Sigma-Aldrich	T62200
Thiourea	Sigma-Aldrich	T8656
Tris-hydrochloride (Tris-HCl)	Sigma-Aldrich	T3253
Triton X-100	Sigma-Aldrich	T8787
Trizma base	Sigma-Aldrich	T1503
Tween-20	Sigma-Aldrich	P7949
Urea	Sigma-Aldrich	U1250
2.Enzymes		
α2-3,6,8,9-neuroaminidase (Sialidase)	EDM Millipore	362280 (KP0012)
β1,4-galactosidase	EDM Millipore	362280 (KP0004)
β-N-acetylglucosaminidase	EDM Millipore	362280 (KP0013)
Chrondroitinase ABC	Sigma-Aldrich	C3667
Endo-α-N-acetylgalactosaminidase (O-glycosidase)	EDM Millipore	362280 (KP0011)
Heparinase II	Sigma-Aldrich	H6512
Keratanase	Sigma-Aldrich	G6920
PNGaseF (N-Glycosidase)	EDM Millipore	362280 (KP0001)
Trypsin	Thermo Scientific	90057
3.Reagent kits		
NuPAGE Novex BisTris Acrylamide gels	Thermo Scientific	NP0322PK2
Pierce BCA Protein Assay kit	Thermo Scientific	23227
miRNeasy Mini kit	Qiagen	4053228006220

TaqMan Probes

Species	Target	Assay
Mouse	*Vcan*	Mm01283063_m1
Mouse	*Acan*	Mm00545794_m1
Mouse	*Hapln1*	Mm00488952_m1
Mouse	*Adamts1*	Mm01344169_m1
Mouse	*Adamts4*	Mm00556068_m1
Mouse	*Adamts5*	Mm00478620_m1
Mouse	*Tgfb1*	Mm01178820_m1
Mouse	*Tgfb2*	Mm00436955_m1
Mouse	*Tgfb3*	Mm00436960_m1
Mouse	*Tgfbr1*	Mm00436964_m1
Mouse	*Tgfbr2*	Mm03024091_m1
Mouse	*Tgfbr3*	Mm00803538_m1
Mouse	*Actb*	Mm00607936_s1
Human	*VCAN*	Hs00171642_m1
Human	*GAPDH*	Hs02786624_g1
Human	*ADAMTS1*	Hs00199608_m1
Human	*ADAMTS4*	Hs00192708_m1
Human	*ADAMTS5*	Hs00199841_m1
Human	*LRP1*	Hs00233856_m1
Human	*ACTB*	Hs99999903_m1

SUPPLEMENTAL MATERIAL

Role of ADAMTS-5
in Aortic Dilatation and Extracellular Matrix Remodeling

Marika Fava[1,2,3], Javier Barallobre-Barreiro[1], Ursula Mayr[1], Ruifang Lu[1], Athanasios Didangelos[1], Ferheen Baig[1], Marc Lynch[1], Norman Catibog[1], Abhishek Joshi[1], Temo Barwari[1], Xiaoke Yin[1], Marjan Jahangiri[2], Manuel Mayr[1,3]

[1] King's British Heart Foundation Centre, King's College London, London, UK
[2] St George's University of London, NHS Trust, London, UK
[3] Cardiovascular Research Center, Icahn School of Medicine at Mount Sinai, New York, US

Address for correspondence:
Manuel Mayr, MD, PhD, King's British Heart Foundation Centre, King's College London, London, UK Telephone: +44-20 7848 5446, Fax: 020 7848 5298, Email: manuel.mayr@kcl.ac.uk

ONLINE METHODS

In vitro metalloprotease digestion assay. Murine aortic specimens were dissected into smaller pieces and washed 5 times in ice-cold, 1X PBS. The tissue blocks were then mixed with 10 volumes metalloprotease reaction buffer (10mM $CaCl_2$, 120mM NaCl and 50mM Trizma base, pH 7.5), which was either used neat (control) or supplemented with different concentrations (50-100pM) of recombinant proteins; murine ADAMTS-1 and murine ADAMTS-5, all purchased from R&D Systems. The samples were incubated for 24hrs at 37°C. Subsequently, the released proteins in the tissue supernatants were deglycosylated. For protein deglycosylation, samples were resuspended in deglycosylation buffer (150mM NaCl, 50mM sodium acetate pH 6.8, 10mM EDTA) for 16hrs at 37°C containing a combination of enzymes for GAG-removal enzymes: chondroitinase ABC (1:100), endo-β1,4-galactosidase (1:500) and heparinase II (1:500). The deglycosylated proteins were separated by gel electrophoresis prior to digestion and LC-MS/MS.

Gel-LC-MS/MS analysis of aortic supernatants. Proteins released from aortas on incubation with ADAMTS-1 and ADAMTS-5 were first separated by SDS-PAGE. Sample buffer (100mM Tris pH 6.8, 40% glycerol, 0.2% SDS, 2% β-mercaptoethanol and 0.02% bromophenol blue) was added to the deglycosylated extracts and boiled at 96°C for 10min prior to separation on 4-12% Bis-Tris gradient gels (Life Technologies, Cat No. EC60385BOX). Electrophoresis was performed at 130-170V for 100-120min in 1x NuPage MOPS SDS Running Buffer (Life Technologies). Proteins were silver-stained for visualization and gel lanes were cut into 10 consecutive pieces. All gel bands were subjected to in-gel digestion with trypsin using an Investigator ProGest (Digilab) robotic digestion system. Tryptic peptides were lyophilized, reconstituted with 0.05% TFA in 2% ACN and separated on a nanoflow LC system (Thermofisher Scientific, Ultimate 3000). Peptides were eluted with a 40-min gradient (10–25% B in 35min, 25–40% B in 5min, 90% B in 10min, and 2%B in 30min where A is 2% ACN, 0.1% formic acid in HPLC H_2O and B is 90% ACN, 0.1% formic acid in HPLC H_2O). The column (Thermofisher Scientific, PepMap C18, 25cm length, 75µm internal diameter, 3µm particle size) was coupled to a nanospray source (Picoview). Spectra were collected from an Orbitrap mass analyzer (LTQ-Orbitrap XL, ThermoFisher Scientific) using full ion scan mode over the mass-to-charge (m/z) range 450–1600. MS/MS was performed on the top six ions in each MS scan using the data-dependent acquisition mode with dynamic exclusion enabled. MS/MS peak lists were generated by extract_msn.exe and matched to a mouse database (SwissProt_57.15, 16230 protein entries) using Mascot (version 2.3.01, Matrix Science). Carbamidomethylation of cysteine was chosen as a fixed modification and oxidation of methionine, lysine and proline were chosen as a variable modifications. The mass tolerance was set at 10ppm for the

precursor ions and 0.8Da for fragment ions. Up to two missed cleavages were allowed. Scaffold (version 3.0.08, Proteome Software Inc., Portland, OR) was used to calculate the spectral counts and to validate MS/MS-based peptide and protein identifications. Peptide identifications were accepted if they could be established at greater than 95.0% probability. Protein identifications were accepted if they could be established at a minimum of 99.0% probability.

ECM protein extraction. Diced tissue was weighed (8-12mg) and immediately placed into Eppendorf tubes containing 1 ml of ice-cold PBS supplemented with 1:100 (v:v) of a broad-spectrum protease inhibitor cocktail (Sigma-Aldrich), and 25mM EDTA to ensure inhibition of metalloproteinases. After 5 washes with PBS buffer the diced samples were incubated with a 0.5M NaCl buffer supplemented with 10mM Tris at pH 7.5, 1:100 (v:v) of a proteinase inhibitor cocktail and 25mM EDTA. The volume of the buffer was adjusted to 5:1 (v:w). Samples were mildly vortexed for 2hrs at room temperature (RT) to solubilize loosely bound ECM and ECM-associated proteins, after which the NaCl buffer was collected and frozen for later use. Samples were washed briefly in the PBS buffer, followed by incubation with 0.08% sodium dodecyl sulphate (SDS) supplemented with proteinase inhibitor cocktail and 25mM EDTA (same ratios as for NaCl buffer above). Samples were mildly vortexed for 2hrs at RT to achieve removal of cellular components, taking particular care to ensure a low vortexing speed to avoid mechanical disruption of the ECM. SDS extracts were then collected and frozen for later use. The tissue samples were washed briefly with water. Finally, the samples were incubated in 4M guanidine hydrochloride buffer (GuHCl) supplemented with 50mM sodium acetate at pH 5.8, 1:100 (v:v) of a proteinase inhibitor cocktail and 25mM EDTA. The volume of the buffer was adjusted to 5:1 (v:w) and the incubation was performed for 48hrs at RT. GuHCl destabilises the ionic, disulfide-dependent protein conformations in large aggregating proteoglycans (PGs), small PGs, cell attachment matrix glycoproteins, fibronectins and laminins and basement membrane components. A vigorous vortexing speed was used to enhance mechanical disruption of the ECM components at this stage. GuHCl extracts were collected and protein concentration was measured by spectrophotometry based on the absorbance at 280nm.

Deglycosylation of ECM extracts. After extraction, 15µg of protein from GuHCl extracts were incubated with 100% ethanol (1:10 volume ratio) at -20°C overnight. After incubation, proteins were precipitated by centrifugation at 16,000 g for 1h at 4°C. Supernatants were carefully removed and protein pellets were dried using a vacuum centrifuge (ThermoFisher Scientific). Precipitation ensures removal of GuHCl, which would interfere with later steps (i.e. enzymatic digestions). For protein deglycosylation (i.e. removal of glycans attached to proteins), a two-step protocol was pursued. In the first step, samples were resuspended in deglycosylation buffer (0.2mol/L Tris, 0.2mol/L sodium acetate,

0.1mol/L EDTA, 0.05mol/L sodium phosphate, pH 6.8) containing a combination of enzymes for glycosaminoglycan (GAG)-removal (as mentioned above) and three additional enzymes that ensure debranching of sugar residues: α2-3,6,8,9-Neuraminidase (from *Arthrobacter ureafaciens*), which cleaves all non-reducing terminal branched and unbranched sialic acids; β1,4-Galactosidase (from *Streptococcus pneumonia*) releases only β1,4-linked, non-reducing terminal galactose from complex carbohydrates and glycoproteins; β-N-Acetylglucosaminidase (from *Streptococcus pneumonia*) cleaves all non-reducing terminal β-linked N-acetylglucosamine residues from complex carbohydrates and glycoproteins (all purchased from Merck-Millipore and used at a ratio of 1:200). Endo-α-N-acetylgalactosaminidase (O-glycosidase from *Streptococcus pneumoniae*) was added to ensure removal of O-glycosylation. This enzyme cleaves serine- or threonine-linked unsubstituted Galβ1,3GalNAc. The samples were incubated for 1h at 25°C and 24hrs at 37°C, at 200rpm. Removal of sugar monomers facilitates the later cleavage by PNGase-F. This enzyme cleaves all asparagine-linked oligosaccharides unless α1,3-core fucosylated. Importantly, asparagine must be peptide-bonded at both termini. After the first incubation step, water was evaporated from the extracts and substituted for an equal amount of $H_2^{18}O$ containing 1:100 PNGase-F (N-glycosidase F). Subsequently, samples were incubated under constant agitation, at 37°C for 48hrs. Deglycosylation in the presence of $H_2^{18}O$, ensures labelling of asparagines with ^{18}O every time a deglycosylation event takes place. During LC-MS/MS analysis, detection of ^{18}O in deamidated asparagines is an indirect indicator of the presence of N-glycosylation.

In-solution digestion and C18 clean-up of ECM extracts. Deglycosylated GuHCl extracts were denatured by the addition of 9M urea, 3M thiourea (final conc. 6M urea, 2M thiourea), and reduced by the addition of 100mM DTT (final conc. 10mM) followed by incubation at 37°C for 1h, 240rpm. The samples were then cooled down to RT before being alkylated by the addition of 500mM iodoacetamide (final conc. 50mM) followed by incubation in the dark for 1h. Pre-chilled (-20°C) acetone (8x volume) was used to precipitate the samples overnight at -20°C. Samples were centrifuged at 14,000 g for 25min at 4°C and the supernatant subsequently discarded. Protein pellets were dried using a speed vac (Thermo Scientific, Savant SPD131DDA), re-suspended in 0.1M TEAB buffer, pH 8.2, containing trypsin (Cat No. 90057, Thermo Scientific; 1:50, trypsin:protein) and digested overnight at 37°C, 240rpm. The digestion was stopped by acidification of the samples with 10% TFA (final concentration 1% TFA). Peptide samples were purified using a 96-well C18 spin plate (Harvard Apparatus). The resin was activated using 200µl methanol and centrifuged at 1,000 g for 1min. Wash steps included 200µl of 80% ACN, 0.1% TFA in H_2O, and three equilibration steps using 200µl of 1% ACN, 0.1% TFA in H_2O with centrifugation (1,000 g for 1min) after each step. Samples were loaded onto the resin and centrifuged at 2,000 g for

1min; the flow-through was reloaded onto the resin a second time and centrifugation repeated. The resin was then washed three times with 200 µl 1% ACN, 0.1% TFA in H_2O (centrifugation at 1,500 g for 1min). Finally, the samples were eluted with 170µl of 50% acetonitrile, 0.1% TFA in H_2O (centrifugation at 1,500 g for 1min); this step was repeated, combining the collected eluate. The eluates were dried using a speed vac (Thermo Scientific, Savant SPD131DDA) and re-suspended in 0.05% TFA in 2% ACN for LC-MS/MS analysis.

Discovery proteomics in ECM extracts. The resuspended peptide samples were separated on a nanoflow LC system (UltiMate 3000 RSLC nano). Samples were injected onto a nano-trap column (Acclaim® PepMap100 C18 Trap, 5mm x 300um, 5µm, 100Å), at a flow rate of 25µL/min for 3min, using 0.1% FA in H_2O. The following nano LC gradient was used to separate the peptides at 0.3µL/min: 0−10min, 4-10% B; 10−75min, 10-30% B; 75-80min, 30−40% B; 80-85min, 40-99%B, 85-89.8min 99%B, 89.8-90min 99-4%B, 90-120min 4% B, where A = 0.1% FA in H_2O, B = 80% ACN, 0.1% FA in H_2O. The nano column (Acclaim PepMap100 C18, 50 cm x 75 µm, 3 µm, 100 Å) was kept at 40°C and coupled to a nanospray source (Picoview, New Objective, US). Spectra were collected from a Q Exactive HF (Thermo Fisher Scientific) using full MS mode (resolution of 60,000 at 200m/z) over the mass-to-charge (m/z) range 350–1600. Data-dependent MS/MS scan was performed using the top 15 ions in each full MS scan (resolution of 15,000 at 200m/z) with dynamic exclusion enabled. Proteome Discoverer (version 2.1.0.81, Thermo Scientific) was used to search raw data files against the mouse data-base (UniProtKB/Swiss-Prot version 2016_02, 16683 protein entries) using Mascot (version 2.3.01, Matrix Science). The mass tolerance was set at 10ppm for precursor ions and 20mmu for fragment ions. Trypsin was used as the enzyme with up to two missed cleavages being allowed. Carbamidomethylation of cysteine was chosen as a fixed modification; oxidation of methionine, lysine and proline, and deamidation of asparagine in the presence of ^{18}O water were chosen as variable modifications. Scaffold (version 4.7.3, Proteome Software Inc., Portland, OR) was used to validate MS/MS-based peptide and protein identifications with the following filters; a peptide probability of greater than 95.0% (as specified by the Peptide Prophet algorithm), a protein probability of greater than 99.0%, and at least two independent peptides per protein. The normalized total ion current (TIC) was used for quantification.

Targeted proteomics in ECM extracts. A Parallel Reaction Monitoring (PRM) method was developed using Skyline software (version 3.6, MacCoss Lab Software). Data from the discovery proteomics analysis were used to select proteotypic peptides of ECM and related proteins. Precursor ions for proteins of interest that were not detected in the untargeted analysis were predicted *in silico* using SRM Atlas. Skyline was used to optimize

retention times. Proteotypic peptides were scheduled using the retention time obtained from test experiments with the same LC configuration and eluting gradient; retention time windows were set at +/- 4min. The same LC and Q Exactive HF system was used as for untargeted analysis but with a 220min LC gradient. After trapping, at a flow rate of 25μL/min for 3min, using 0.1% FA in H_2O, the following nano-LC gradient was applied at 0.3μL/min: 0−20min, 4-8% B; 20−200min, 8-25% B; 200−210min, 25−40% B; 210-215min, 40-99% B, 215-219.8min, 99% B, 219.8-220min, 99-4% B, 220-250min 4% B, where A=0.1% FA in H_2O, B=80% ACN, 0.1%FA in H_2O. Spectra were collected on a Q Exactive HF (ThermoFisher Scientific) in PRM mode (MS/MS resolution of 30,000 at 200m/z). An isolation window of 2.0 m/z, automatic gain control (AGC) values of 2E5 and a maximum injection time of 60ms were used. Fragmentation was performed with a normalized collision energy of 28. MS/MS scans were acquired with a first fixed mass of 110.0m/z. The identity of a specific peptide was confirmed by the presence of multiple fragment ions at the same retention time. The inclusion list is shown in **Supplemental Table III**.

Western blot. Aliquots from GuHCl and total protein extracts were mixed with protein loading buffer and denatured at 98°C for 5-10min before being briefly centrifuged. Protein samples were separated on 4-12% Bis-Tris gradient gels at 130-170V for 100-120min in 1x NuPage MOPs SDS Running Buffer. Subsequently, the samples were transferred to nitrocellulose membranes in ice-cold transfer buffer (25 mM Tris-Base and 200mM Glycine in 20% methanol). Ponceau S red staining was used to ensure efficient transfer and equal loading. Next, membranes were blocked in 5% milk in PBS with 0.1% Tween-20 (PBST) for 1h on a shaker at RT. After a brief wash in PBST, they were incubated overnight with primary antibody solution. Please see the Major Resources Table in the Supplemental Material. The following day, after three washes in PBST (15min each), the membranes were incubated for 1h at RT with the HRP-conjugated secondary antibody diluted in 5% milk in PBST, according to the source of the primary antibody. The membranes were then washed three times in PBST for 15min and developed using ECL western blotting detection reagent using either X-ray films (FUJIFILM) or Chemidoc Touch, Imaging System (BIORAD). Immunoblots were quantified by densitometry using Image-J software.

RNA isolation. RNA extraction was performed using the miRNeasy Mini Kit (Qiagen) following the manufacturers' protocol. For aortic tissue, samples were diced using a scalpel, incubated in 700μl of Qiazol Lysis Reagent and homogenised using FastPrep ceramic lysis beads (Matrix D, MPBio). Cells were washed twice in cold sterile PBS and lysed in 700μl of Qiazol Lysis Reagent. Samples were subsequently incubated at RT for 5min, and then vortexed with 140μl of chloroform. The lysate was then incubated for a further 5min at RT before being centrifuged for 15min at 12,000 g, at 4°C. 280μl of the upper aqueous phase

were transferred to a new tube, mixed with 1.5 volumes of 100% ethanol and transferred into a miRNeasy mini column. The remaining centrifugation steps were carried out at RT. The column was centrifuged for 1min at 12,000 g and the flow through was discarded, next 700µl of RWT buffer was added to the column, centrifuged for 1min at 12,000 g and the flow through was discarded. Next, 500µl of RPE buffer were added to the column before a further centrifugation step for 1min at 12,000 g. The flow through was discarded and a further 500µl of RPE buffer were added to the column before it was centrifuged at 12,000 g for 2min. The columns were transferred to clean collection tubes and centrifuged at 15,000 g for 1min, before being transferred to a new tube. The RNA was eluted with 30µl of RNase-free water, by centrifugation at 10,000 g for 1min. RNA concentration (Abs 260nm) and purity (260/280) were measured in 1µl using spectrophotometry (NanoDrop ND-1000, ThermoScientific). Integrity of RNA was evaluated using Agilent Bioanalyser System. RNA quality was considered acceptable if the RNA integrity number (RIN) was above 7.

Reverse transcription (RT) and quantitative real-time PCR (qPCR). The RNA was reverse-transcribed using random hexamers with SuperScript VILO MasterMix (Invitrogen) according to manufacturers' protocol, with sample preparation being performed on a StarChill PCR rack to maintain low temperature. RNA concentration of samples was adjusted to contain equal amounts of RNA (250-500ng) in 8µl using RNase-free water. No DNase treatment was performed. The reverse transcription reaction was set up by mixing the 8µl of RNA with 2µl of SuperScript VILO MasterMix. RT reaction was performed in a Veriti thermal cycler (Applied Biosystems) with the following protocol: incubation at 25°C for 10min followed by 2hrs incubation at 42°C. the reaction was terminated by incubation at 85°C for 5min. Samples were kept at 4°C for immediate use in the qPCR reaction or stored at -20°C.

The RT product was diluted 1:15 to 1:25 using RNase-free water. TaqMan assays using hydrolysis probes (Major Resources Tables) were used for quantitative PCR (qPCR). 2.25µl of diluted RT product were combined with 2.5µl of TaqMan Universal PCR Master Mix, no AmpErase UNG (Applied Biosystems), 0.25µl of TaqMan assays on a MicroAmp Optical 384-well reaction plate, using a Bravo Liquid Handling Platform (Agilent). qPCR reaction was performed in a ViiA 7 Real-Time PCR System (Applied Biosystems), set to run as follows: incubation at 95°C for 10min, followed by 40 cycles of 95°C for 15sec and 60°C for 1min. Data was analysed using ViiA 7 software (Applied Biosystems). A minimum of two reference genes was used throughout the study and stability of RNA isolation, RT and qPCR was determined by variability of and correlation between reference genes. Relative amounts of the targets were calculated using the $2^{-\Delta\Delta Cq}$ method,[17] with statistical analysis performed on ΔCq values.

Supplemental Table I. Extracellular proteins released from mouse aortas on incubation with ADAMTS-1 or ADAMTS-5.

Identified Proteins	Uniprot Accession	M_r (kDa)	Control	ADAMTS-1	ADAMTS-5	P-value
ADAMTS-1	P97857	106	0±0	42.5±0.4	0±0	**0.036**
ADAMTS-5	Q9R001	102	0±0	0±0	15.9±8.4	**0.036**
Adipocyte enhancer-binding protein 1	Q640N1	128	24.0±5.4	23.4±1.9	27.2±0.8	0.339
Adiponectin	Q60994	27	2.4±2.2	5.5±2.2	0.6±1.1	0.079
Aggrecan	Q61282	222	0±0	0±0	0.6±1.1	>0.999
Agrin	A2ASQ1	208	0±0	3.3±1.5	3.2±3.0	0.186
Alpha-2-HS-glycoprotein	P29699	37	4.8±2.3	3.6±0.6	2.6±2.2	0.543
Annexin A2	P07356	39	7.7±6.8	12.0±3.0	17.5±4.5	0.100
Apolipoprotein A-I	Q00623	31	0±0	1.0±1.7	0±0	>0.999
Apolipoprotein A-IV	P06728	45	0.8±1.4	0±0	0±0	>0.999
Beta-2-glycoprotein 1	Q01339	39	10.7±2.8	6.5±1.5	6.5±0.6	0.071
Biglycan	P28653	42	6.0±3.4	6.5±1.5	7.1±2.9	0.929
Cell surface glycoprotein MUC18	Q8R2Y2	72	7.7±1.8	9.7±1.0	8.1±1.5	0.296
Chondroitin sulfate proteoglycan 4	Q8VHY0	252	46.5±12.1	34.4±2.1	40.4±4.8	0.132
Clusterin	Q06890	52	0±0	1.6±2.8	0±0	>0.999
Collagen alpha-1(I)	P11087	138	3.3±1.2	3.2±1.1	2.6±2.5	0.132
Collagen alpha-1(III)	P08121	139	7.9±1.7	8.8±0.9	5.5±0.5	**0.050**
Collagen alpha-1(VI)	Q04857	108	83.1±6.3	84.1±4.9	89.9±5.8	0.361
Collagen alpha-1(XII)	Q60847	340	7.6±4.0	15.9±1.1	15.9±5.7	0.100
Collagen alpha-1(XIV)	Q80X19	193	68.2±19.5	78.6±3.6	70.5±7.8	0.511
Collagen alpha-1(XV)	O35206	140	42.7±5.7	43.5±3.5	37.5±4.0	0.339
Collagen alpha-1(XVIII)	P39061	182	37.2±3.7	38.0±2.4	36.5±5.3	0.829
Collagen alpha-2(I)	Q01149	130	3.0±2.6	3.9±1.0	3.9±0	0.929
Collagen alpha-2(IV)	P08122	167	1.2±2.1	2.0±3.4	1.6±2.8	>0.999
Collagen alpha-2(VI)	Q02788	110	35.6±3.4	47.1±5.9	47.5±6.3	0.071
Collagen alpha-6(VI)	Q8C6K9	246	18.2±2.2	30.2±4.7	34.9±5.2	**0.025**
Decorin	P28654	40	1.7±1.5	2.3±2.0	2.9±2.9	0.593
Extracellular superoxide dismutase [Cu-Zn]	O09164	27	38.5±11.3	43.5±6	44.3±2.4	0.829
Fibromodulin	P50608	43	0±0	2.0±3.4	1.9±1.9	0.679
Fibronectin	P11276	272	48.0±4.4	56.2±10.9	89.6±10.7	**0.025**
Fibulin-2	P37889	132	1.6±2.8	1.6±2.8	7.4±7.7	0.071
Fibulin-5	Q9WVH9	50	32.5±3.5	32.4±4.7	33.7±2.2	0.879
Integrin alpha-5	P11688	115	0±0	0±0	1.0±1.7	>0.999
Integrin alpha-IIb	Q9QUM0	113	19.4±4.1	1.6±2.8	0±0	**0.036**
Integrin beta-1	P09055	88	5.0±0.9	2.0±2.0	0.6±1.1	**0.025**
Integrin beta-3	O54890	87	7.9±1.1	0.7±1.1	0±0	**0.036**
Laminin subunit alpha-2	Q60675	343	1.8±3.1	4.9±1.7	6.5±2.1	0.132
Laminin subunit alpha-4	P97927	202	1.4±2.5	3.6±3.1	2.6±2.2	0.529
Laminin subunit beta-1	P02469	197	0.7±1.2	4.9±2.5	5.2±3.4	0.132
Laminin subunit beta-2	Q61292	196	23.8±2.7	24.4±1.9	19.7±2.5	0.139
Laminin subunit gamma-1	P02468	177	25.0±5.0	20.4±4.3	24.6±1.6	0.339
Latent-TGFβ-binding protein 1	Q8CG19	187	1.7±1.5	1.0±1.7	4.9±1.0	0.068
Latent-TGFβ-binding protein 4	Q8K4G1	179	120.8±21.	123.7±10.1	130.9±17.7	0.629
Lumican	P51885	38	14.7±2.3	21.1±2.6	17.5±2.6	**0.025**
Microfibril-associated glycoprotein 4	Q9D1H9	29	1.6±2.8	0±0	0±0	>0.999
Mimecan	Q62000	34	7.0±0.8	10.0±3.8	10.7±1.7	**0.050**
Periostin	Q62009	93	28.6±5.6	27.3±2.4	26.9±1.6	0.993
Perlecan	Q05793	398	126.5±13	131.5±1.1	129.4±7.2	0.721
Prolargin	Q9JK53	43	2.2±3.8	7.2±3.2	5.8±4.2	0.357
Prolow-density lipoprotein receptor-related protein 1	Q91ZX7	505	4.6±1.4	6.2±1.1	8.1±0.6	**0.011**
Tenascin	Q80YX1	232	1.1±1.8	2.9±1.0	1.3±2.3	0.400
TGFβ-induced protein ig-h3	P82198	75	5.2±1.2	9.1±0.6	8.4±3.1	0.139
Thrombospondin-1	P35441	130	17.5±2.9	13.6±1.9	7.4±3.7	**0.011**
Versican	Q62059	367	0±0	5.2±0.6	4.5±1.1	**0.025**
vWF A domain-containing protein 5A	Q99KC8	87	5.6±1.2	9.4±1.9	11±3.9	0.071

Values are normalised Total Spectral counts (Av±SD). *P*-values for changes among the different groups (n=3) were identified by Kruskal-Wallis test. Results in bold indicate *P* < 0.05. Values are average (Av) normalised total spectra ± standard deviation (SD). Control: incubation in buffer only.

Supplemental Table II. ECM-related proteins in murine aortas of AngII-treated Adamts5$^{+/+}$ and Adamts5$^{\Delta cat}$ mice.

Identified proteins	Uniprot accession	Mr (kDa)	Total spectra	Unique spectra	Unique peptides	Sequence coverage	Fold change	*P*-value
Adiponectin	ADIPO	27	14	4	4	9.7	NA	NA
Aggrecan core protein	PGCA	222	328	54	34	17.0	1.10	0.662
Agrin	AGRIN	208	87	21	19	10.6	1.15	0.792
Alpha-2-HS-glycoprotein	FETUA	37	15	10	8	31.9	NA	NA
Amyloid beta A4 protein	A4	87	74	20	17	20.3	0.60	0.429
Annexin A2	ANXA2	39	129	25	19	47.2	1.53	0.126
Apolipoprotein A-I	APOA1	31	91	17	12	42.4	1.60	0.247
Apolipoprotein A-IV	APOA4	45	31	10	10	19.2	1.35	0.794
Apolipoprotein C-III	APOC3	11	7	5	3	50.5	NA	NA
Apolipoprotein E	APOE	36	56	19	13	43.4	3.32	0.420
Asporin	ASPN	43	292	44	22	55.8	1.05	0.571
Basal cell adhesion molecule	BCAM	68	157	30	23	35.7	0.69	0.082
Beta-2-glycoprotein 1	APOH	39	118	23	17	60.6	2.06	0.082
Biglycan	PGS1	42	845	90	31	66.9	1.05	0.792
Cadherin-13	CAD13	78	43	6	6	9.5	1.20	0.662
Cathepsin B	CATB	37	9	3	3	9.1	NA	NA
Cathepsin D	CATD	45	50	9	6	23.9	1.34	0.429
Chondroitin sulfate proteoglycan 4	CSPG4	252	18	9	9	5.2	NA	NA
Chymase	CMA1	28	53	9	8	33.6	1.02	0.792
Clusterin	CLUS	52	167	30	21	49.1	1.57	0.266
Collagen alpha-1(I) chain	CO1A1	138	4768	269	114	76.0	0.87	0.355
Collagen alpha-1(II) chain	CO2A1	142	125	13	10	10.1	0.93	0.662
Collagen alpha-1(III) chain	CO3A1	139	756	114	62	52.8	0.54	0.931
Collagen alpha-1(IV) chain	CO4A1	161	135	28	14	10.8	0.86	0.792
Collagen alpha-1(V) chain	CO5A1	184	248	31	24	13.8	0.73	0.247
Collagen alpha-1(VI) chain	CO6A1	108	247	53	35	33.4	0.66	0.178
Collagen alpha-1(XI) chain	COBA1	181	25	7	6	4.2	NA	NA
Collagen alpha-1(XII) chain	COCA1	340	37	23	22	9.5	3.80	0.446
Collagen alpha-1(XIII) chain	CODA1	73	2	2	2	8.7	NA	NA
Collagen alpha-1(XIV) chain	COEA1	193	55	19	18	8.9	1.13	0.922
Collagen alpha-1(XV) chain	COFA1	140	162	25	17	14.9	1.08	0.931
Collagen alpha-1(XVIII) chain	COIA1	182	427	56	35	23.7	0.94	0.537
Collagen alpha-2(I) chain	CO1A2	130	2855	210	91	71.6	0.96	0.792
Collagen alpha-2(IV) chain	CO4A2	167	80	19	14	9.0	0.83	0.792
Collagen alpha-2(V) chain	CO5A2	145	457	62	43	41.3	1.33	0.178
Collagen alpha-2(VI) chain	CO6A2	110	220	48	27	34.8	0.51	0.139
Collagen alpha-3(IV) chain	CO4A3	162	2	2	2	1.9	NA	NA
Collagen alpha-6(VI) chain	CO6A6	246	65	20	20	10.6	0.26	0.121
Connective tissue growth factor	CTGF	38	73	17	15	44.3	0.81	0.623
Decorin	PGS2	40	721	84	34	73.2	1.21	0.126
Dermatopontin	DERM	24	125	21	10	53.7	1.11	0.329
Dystroglycan	DAG1	97	26	7	5	4.8	1.61	0.305
Elastin	ELN	72	67	12	10	21.4	0.63	0.126
EMILIN-1	EMIL1	108	21	9	9	5.2	0.86	0.794
Extracellular matrix protein 1	ECM1	63	21	6	6	10.0	0.96	0.100
Extracellular superoxide dismutase	SODE	27	268	40	16	74.1	1.04	0.931
Fibrillin-1	FBN1	312	62	18	17	8.1	0.69	0.881
Fibromodulin	FMOD	43	83	17	10	36.2	1.14	0.792
Fibronectin	FINC	273	1424	244	124	58.6	1.00	0.792
Fibulin-2	FBLN2	132	2	2	2	2.5	NA	NA
Fibulin-5	FBLN5	50	151	21	15	38.8	0.76	0.429
Galectin-1	LEG1	15	121	17	9	48.1	1.38	0.056
Galectin-3	LEG3	28	68	11	7	31.1	1.56	0.178
Galectin-3-binding protein	LG3BP	64	5	5	5	14.2	NA	NA
Hyaluronan and proteoglycan link protein 1	HPLN1	40	24	9	8	22.2	NA	NA
Kininogen-1	KNG1	73	4	4	4	11.5	NA	NA
Lactadherin	MFGM	51	372	53	27	60.9	1.03	>0.99
Laminin subunit alpha-2	LAMA2	344	14	8	8	2.1	NA	NA
Laminin subunit alpha-4	LAMA4	202	83	18	18	9.6	1.09	0.931

Laminin subunit alpha-5	LAMA5	404	77	20	19	6.0	1.01	0.792
Laminin subunit beta-1	LAMB1	197	5	5	5	2.5	NA	NA
Laminin subunit beta-2	LAMB2	197	224	46	37	20.0	1.06	0.792
Laminin subunit gamma-1	LAMC1	177	201	41	35	20.8	1.03	0.931
Latent-TGF β-binding protein 1	LTBP1	187	63	12	11	6.4	0.96	0.792
Latent-TGF β-binding protein 2	LTBP2	196	16	7	7	4.6	NA	NA
Latent-TGF β-binding protein 4	LTBP4	179	247	49	37	21.6	0.86	0.537
Lumican	LUM	38	575	66	28	72.8	1.38	0.056
Matrix Gla protein	MGP	12	6	3	2	23.1	NA	NA
Metalloproteinase inhibitor 3	TIMP3	24	20	5	5	20.9	1.27	0.790
Microfibril-associated glycoprotein 4	MFAP4	29	112	18	9	43.6	1.17	0.429
Microfibrillar-associated protein 5	**MFAP5**	**19**	**112**	**13**	**6**	**37.8**	**1.78**	**0.030**
Mimecan	MIME	34	494	54	27	58.7	1.26	0.247
Nephronectin	NPNT	61	137	22	15	28.7	0.69	0.052
Nidogen-1	NID1	137	285	54	41	32.4	1.12	0.329
Nidogen-2	NID2	154	160	37	27	16.5	1.02	0.972
Periostin	POSTN	93	503	94	53	51.3	0.75	0.429
Perlecan	PGBM	398	1810	271	148	46.4	0.91	0.537
Prolargin	PRELP	43	455	51	26	77.8	1.33	0.178
Prolow-density lipoprotein receptor-related protein 1	LRP1	505	28	13	12	2.55	NA	NA
Prosaposin	SAP	61	39	9	7	19.2	1.54	0.429
Protein S100-A10	S10AA	11	38	7	5	52.6	2.30	0.080
Protein S100-A11	S10AB	11	9	3	2	27.6	NA	NA
Protein S100-A4	S10A4	12	8	5	3	20.8	NA	NA
Sclerostin	SOST	23	27	5	4	18.0	0.73	0.329
Serine protease HTRA1	HTRA1	51	308	41	24	49.2	0.79	0.792
Serine protease HTRA3	HTRA3	49	35	12	10	20.9	1.09	>0.99
SPARC	SPRC	34	17	5	5	12.6	0.65	0.550
Tenascin	TENA	232	277	70	59	27.2	0.94	0.792
TGF-β1	TGFB1	44	9	9	9	37.9	NA	NA
TGF-β2	TGFB2	48	19	4	3	12.1	2.10	0.268
TGF-β3	TGFB3	47	4	2	2	6.1	NA	NA
TGF β-induced protein ig-h3	BGH3	75	91	24	18	31.0	0.66	0.429
Thrombospondin type-1 domain-containing protein 4	THSD4	113	87	15	13	13.7	0.85	0.662
Thrombospondin-1	TSP1	130	23	10	10	10.9	2.93	>0.99
Tubulointerstitial nephritis antigen-like	TINAL	53	264	49	27	66.5	1.02	0.931
Vascular cell adhesion protein 1	VCAM1	81	3	3	3	5.4	NA	NA
Versican	**CSPG2**	**367**	**112**	**20**	**14**	**4.6**	**2.19**	**0.009**
Vitronectin	VTNC	55	139	24	15	37.2	1.90	>0.99
von Willebrand factor A domain-containing protein 1	VWA1	45	59	13	11	38.1	0.71	0.755

Number of samples: WT n=6, KO: n=5 *P* values were derived from unpaired Mann Whitney tests and significant changes (p<0.05) are highlighted in bold. NA denotes "not applicable" (note that every time protein expression in more than 3 samples from both groups was undetectable, the test was not performed). Sequence coverage is given in %.

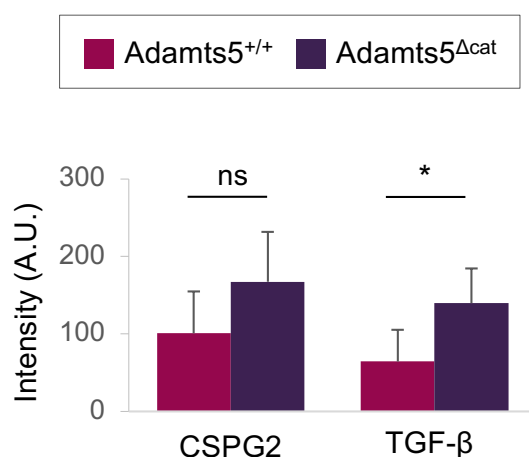**Supplemental Table III**. PRM parameter used for targeted MS analysis of unique peptides from versican.

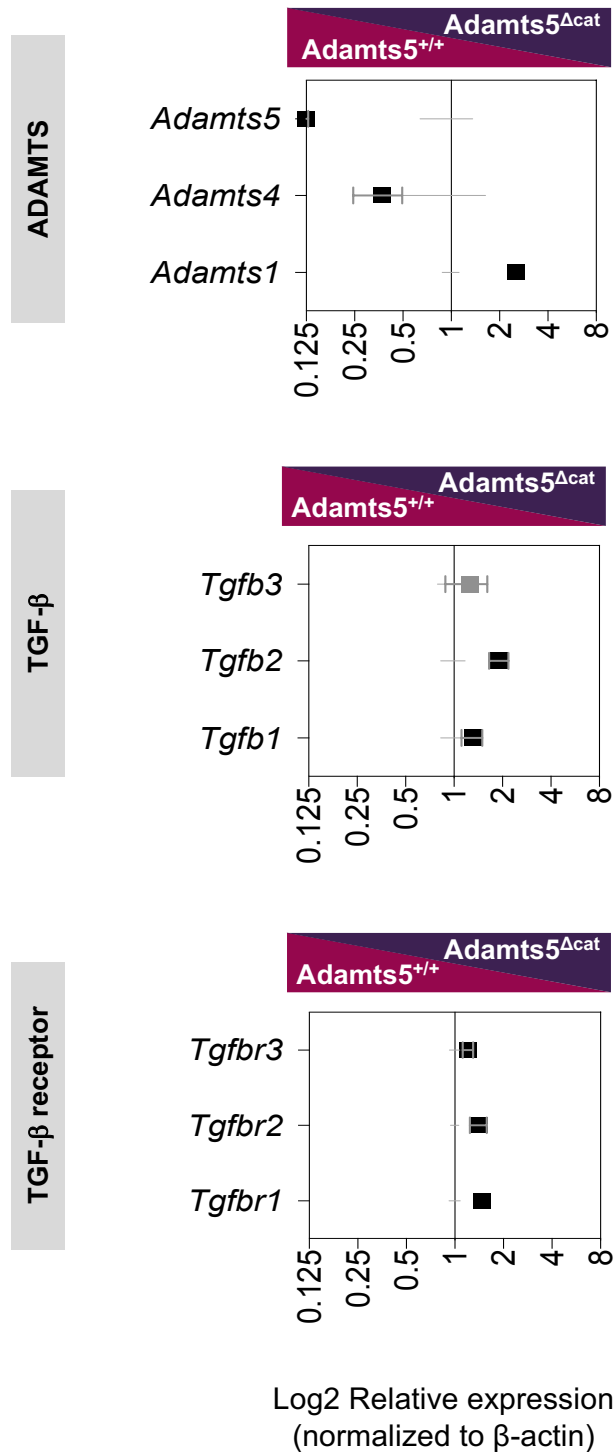| Versican Peptides	Precursor m/z	Precursor z	Product ion	Product ion m/z	Retention time (min)
LATVGELQAAWR (N-terminal)	657.8619	2	y6	744.42	155.1
			y7	873.46	
			y8	930.48	
			y9	1029.55	
			y10	1130.60	
			y11	1201.63	
YEINSLIR (C-terminal)	504.2796	2	y3	401.29	118.1
			y4	488.32	
			y5	602.36	
			y6	715.45	
			y7	844.49	

Supplemental Figure I

Supplemental Figure I. Experimental design. Hypertension was induced by treating 10-week-old Adamts5$^{+/+}$ and Adamts5$^{\Delta cat}$ mice with AngII for 4 weeks. An ultrasound was performed before and after 4 weeks of AngII infusion. Blood pressure measurements were acquired at 3 time points: 2 days before and 5 and 27 days after osmotic mini-pumps for AngII infusion were implanted.
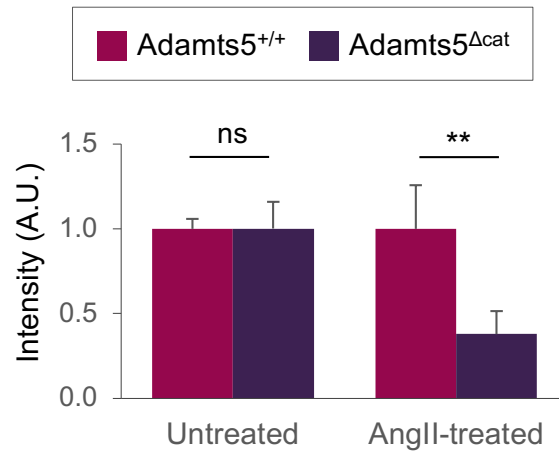
Supplemental Figure II

Supplemental Figure II. Quantification of versican (CSPG2) and TGF-β in the aortas of AngII-treated Adamts5$^{+/+}$ and Adamts5$^{\Delta cat}$ mice by densitometry. Bars represent mean±SD. Statistical significance was calculated using unpaired Student's *t*-test. * denotes P<0.05
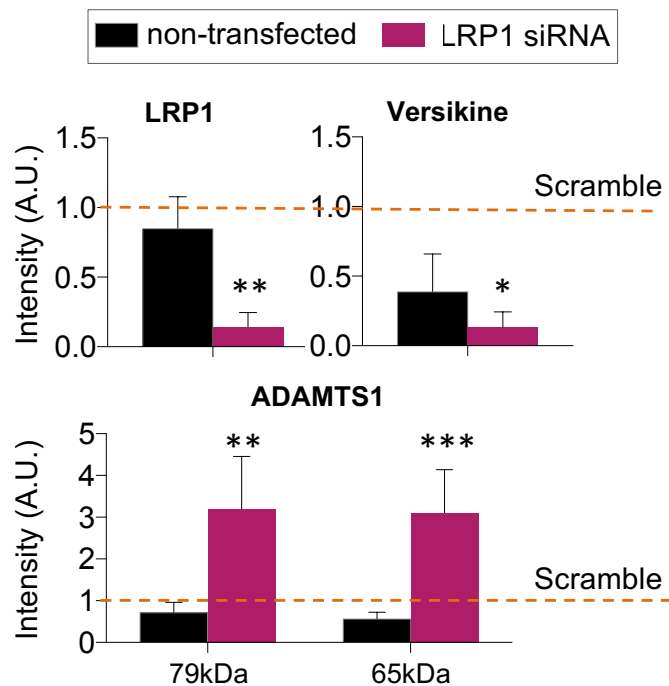
Supplemental Figure III

Supplemental Figure III. Gene expression in murine aortas. Relative gene expression of *Adamts1, 4 and 5*, *Tgfb1, 2 and 3* and *Tgfbr1, 2* and 3 in aortas from untreated Adamts5^{+/+} (n=6) and Adamts5[Δcat] (n=5) mice. β-actin was used as reference gene. Data points are means±SD. Black squares denote *P*<0.05 as determined by Mann-Whitney tests.

Supplemental Figure IV

Supplemental Figure IV. LRP1 in mouse aortas. Quantification of LRP1 in aortas of untreated and AngII-treated Adamts5$^{+/+}$ and Adamts5$^{\Delta cat}$ mice by densitometry. Bars represent means±SD. The intensity values in Adamts5$^{+/+}$ aortas served as reference. Statistical significance was calculated using unpaired Student's *t*-test. ** denotes P<0.01.

Supplemental Figure V

Supplemental Figure V. LRP1 siRNA, protein expression. Quantification of LRP1, the N-terminal fragment of versican (versikine) and the two forms of ADAMTS1 by densitometry. SMCs transfected with scrambled siRNA served as reference. Bars represent mean±SD. Statistical significance was calculated using one-way ANOVA with Dunnett's *post hoc* test. * denotes P<0.05, ** P<0.01, *** P<0.001.